Blessed Plots for the Reversed Horn Current Analysis

J. Evans, J. Hartnell, A. Himmel and D. Naples
for the NuMuBar Group

April 28, 2010
Version 4
(minos-doc-6993-v4)

Document Versions

This document is intended to be a one stop shop that will always have the latest NuMuBar blessed plots in it for the reversed horn current analysis.

Version 1 (minos-doc-6993-v1): Not yet a complete set of figures, but enough to give the document shape. Figures are either in place or there is a placeholder with docdb references as known.

Version 2 (minos-doc-6993-v2): Added more extrapolation and systematics (star) plots. Add ND Data/MC plots.

Version 3 (minos-doc-6993-v3): Added FD Data/MC plots.

Version 4 (minos-doc-6993-v4): FD is updated to 1.75e20 and I added roID and input variables' N-1 plots. ND plots now include the coil hole systematic in the band (energy, trackEn, shower and y) and added the SKZP on/off comparisons.

Brief Overview

The goal of this analysis is to determine the spectrum of $\overline{\nu}_\mu$ events in the FD that will be used to extract physics model parameters. The search for $\overline{\nu}_\mu$ disappearance constrains $\overline{\nu}_\mu \rightarrow \overline{\nu}_\tau$ oscillation parameters. In particular, $\overline{\nu}_\mu$ disappearance will constrain oscillation parameters $\Delta\overline{m}^2$ and $\sin^2(2\overline{\theta}_{23})$ through the measuredoscillation probability,

$$P(\overline{\nu}_\mu \rightarrow \overline{\nu}_\mu) = 1 - \sin^2(2\overline{\theta}_{23}) \sin^2(1.27\Delta\overline{m}^2 \frac{L}{E}).$$

Selection Efficiency and Purity

minos-doc-6984

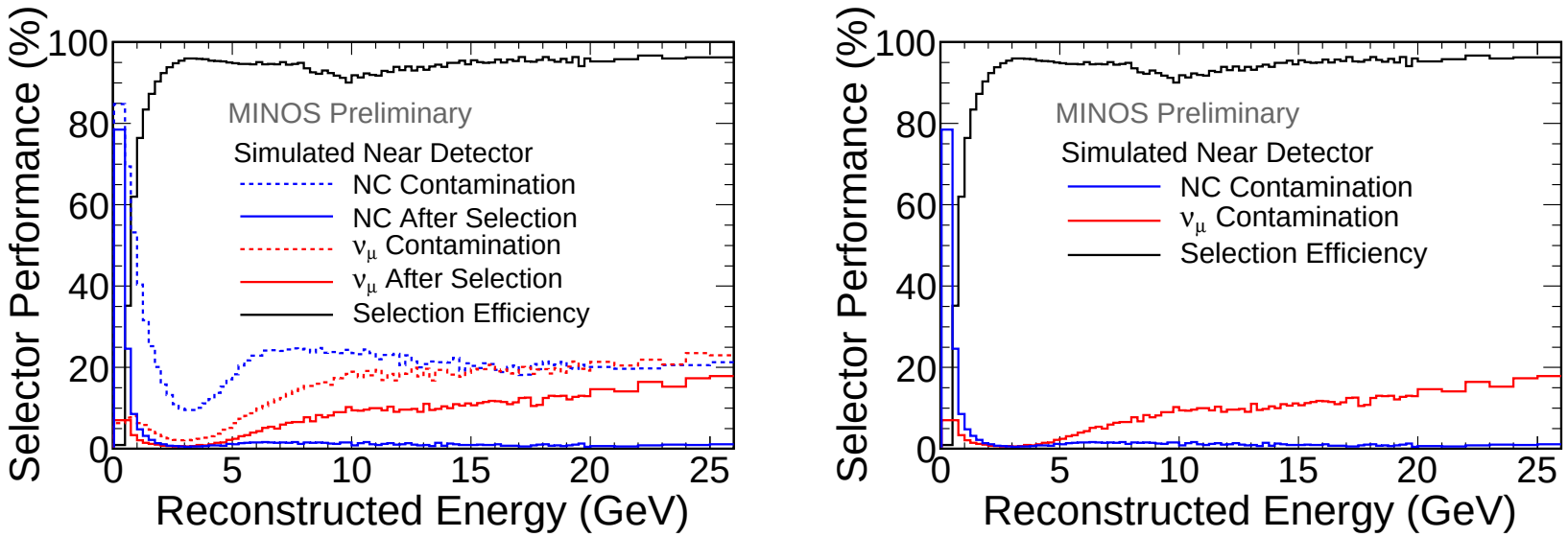

Figure 1: Performance of the current RHC selection ($roID > 0.3$, $qp > 0$) in the near detector, which is essentially the CC selection. The dashed lines show the contamination before selection and the solid show efficiency and contamination after selection. The NuMu contamination rises at higher energies since tracks these do not curve as much and so are more difficult to assign a charge to. minos-doc-6984

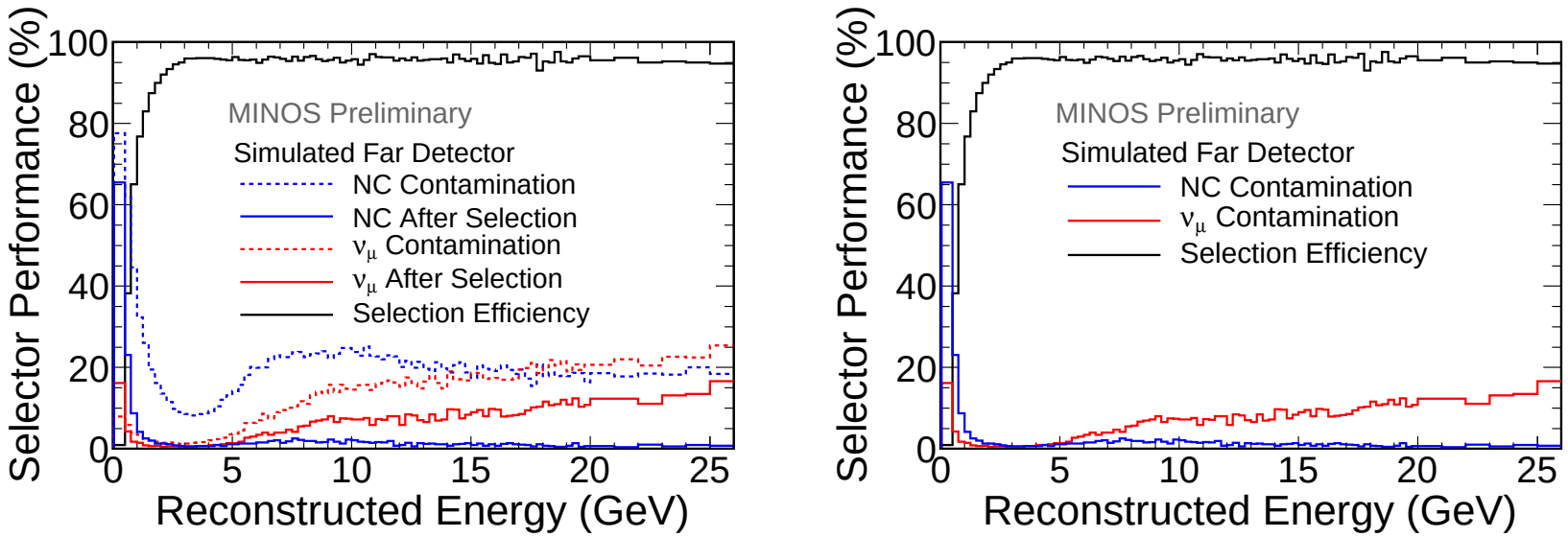

Figure 2: Performance of the current RHC selection ($roID > 0.3$, $qp > 0$) in the far detector, which is essentially the CC selection. The dashed lines show the contamination before selection and the solid show efficiency and contamination after selection. The NuMu contamination rises at higher energies since tracks these do not curve as much and so are more difficult to assign a charge to. minos-doc-6984

ND Data/MC distributions

minos-doc-7177

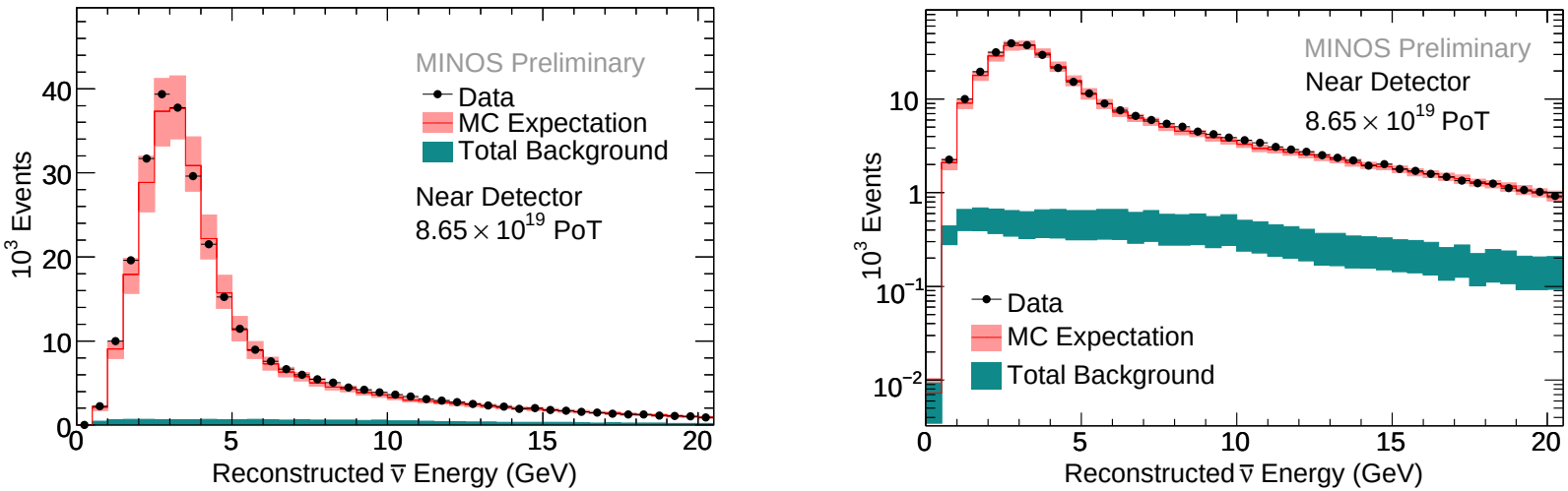

Figure 3: Reconstructed energy distribution of events selected as antineutrinos in the Near Detector. The red histogram represents the Monte Carlo expectation with the systematic error, the blue histogram represents the total (charged and neutral current) background with the background uncertaintiy. Black points represent data. minos-doc-7177

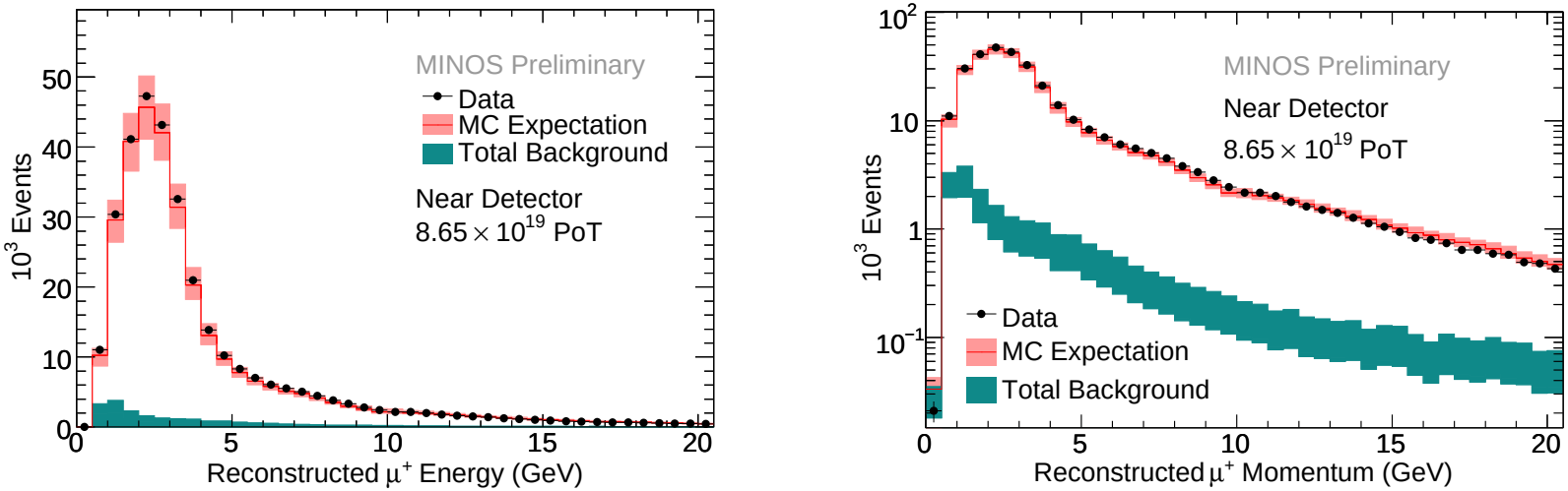

Figure 4: Reconstructed momentum of μ^+ tracks in the Near Detector. The red histogram represents the Monte Carlo expectation with the systematic error, the blue histogram represents the total (charged and neutral current) background with the background uncertaintiy. Black points represent data. minos-doc-7177

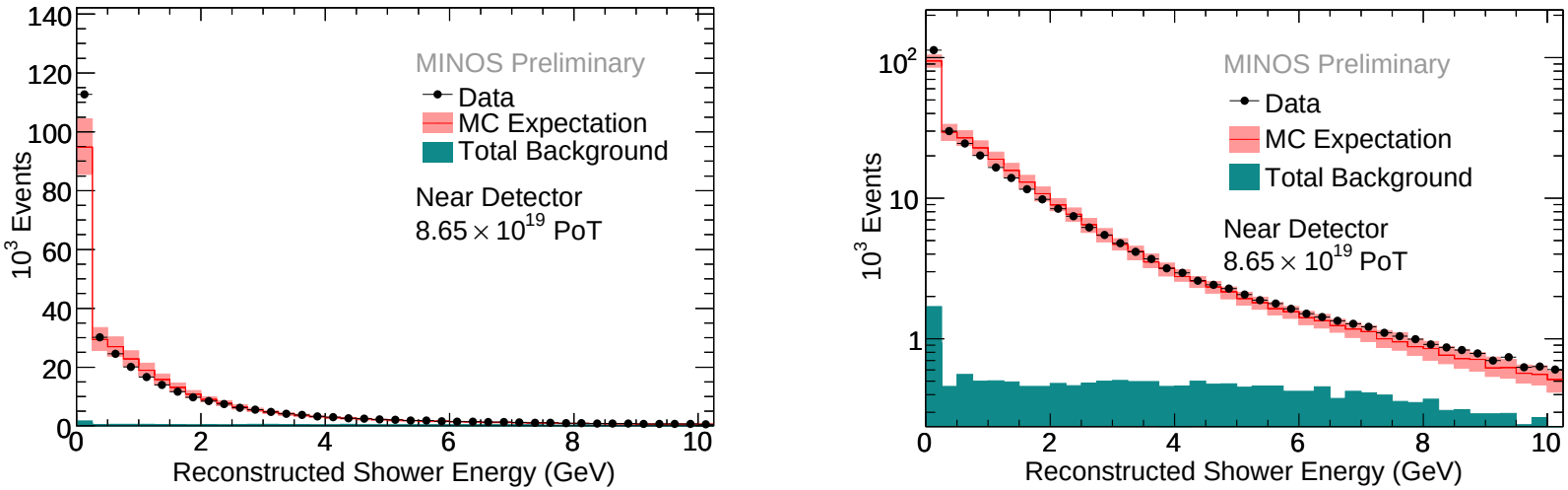

Figure 5: Reconstructed shower energy distribution in the Near Detector. The red histogram represents the Monte Carlo expectation with the systematic error, the blue histogram represents the total (charged and neutral current) background with the background uncertaintiy. Black points represent data. minos-doc-7177

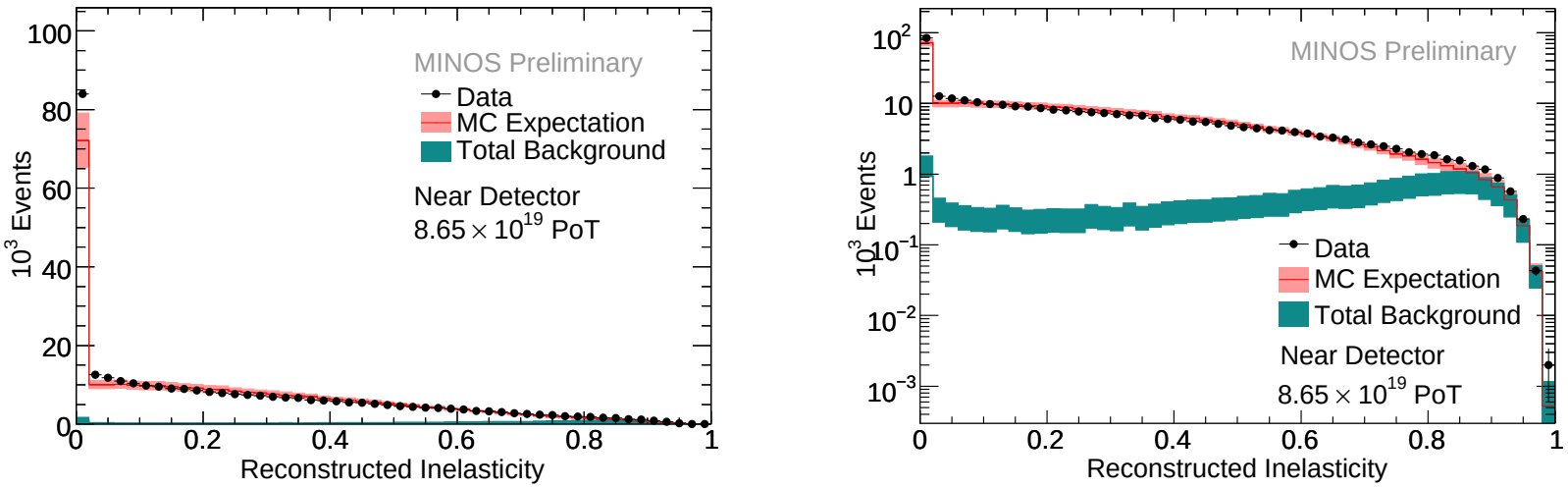

Figure 6: Reconstructed inelasticity distribution in the Near Detector. The red histogram represents the Monte Carlo expectation with the systematic error, the blue histogram represents the total (charged and neutral current) background with the background uncertaintiy. Black points represent data. minos-doc-7177

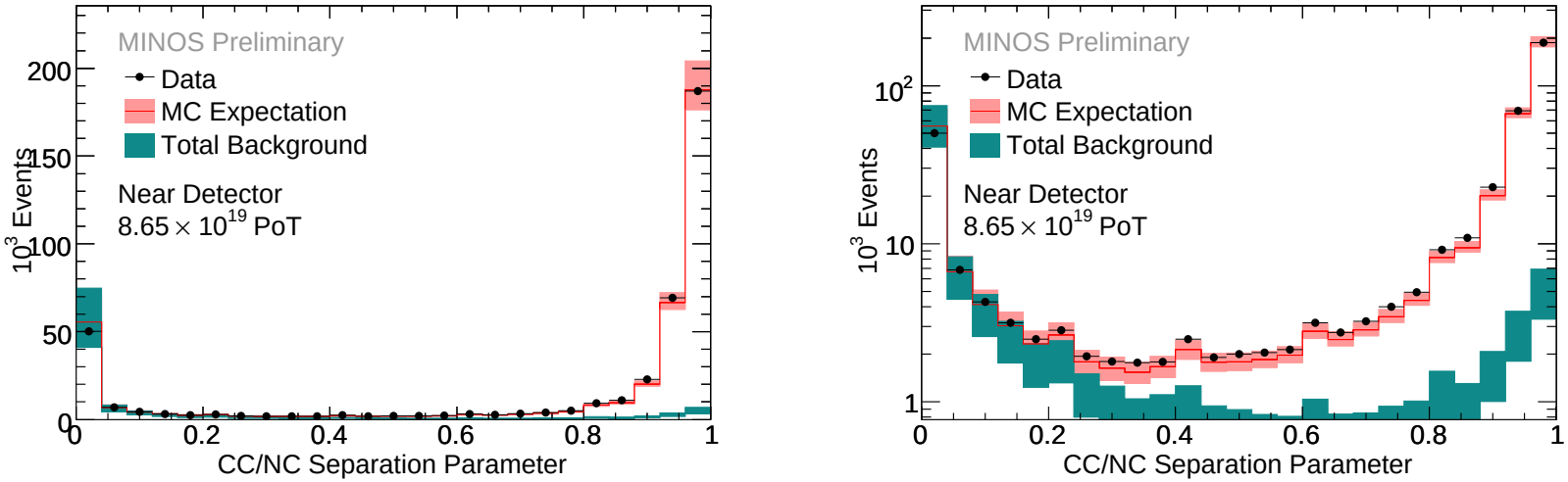

Figure 7: CC/NC separation parameter. The red histogram represents the Monte Carlo expectation with the systematic error, the blue histogram represents the total (charged and neutral current) background with the background uncertaintiy. Black points represent data. The cut removes events with PID< 0.3 minos-doc-7177

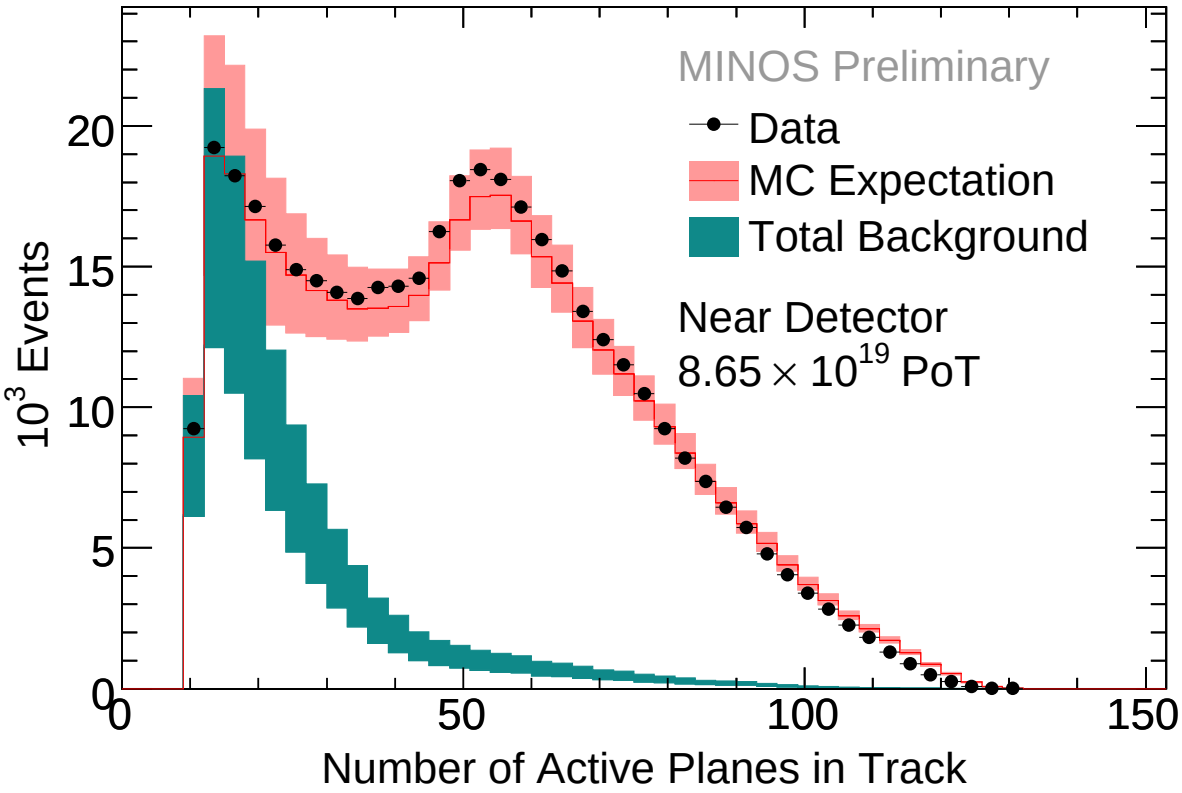

Figure 8: Distribution of PID input variable *number of active scintillator planes in track* before the PID< 0.3 cut is applied. The red histogram represents the Monte Carlo expectation with the systematic error, the blue histogram represents the total (charged and neutral current) background with the background uncertaintiy. Black points represent data. minos-doc-7177

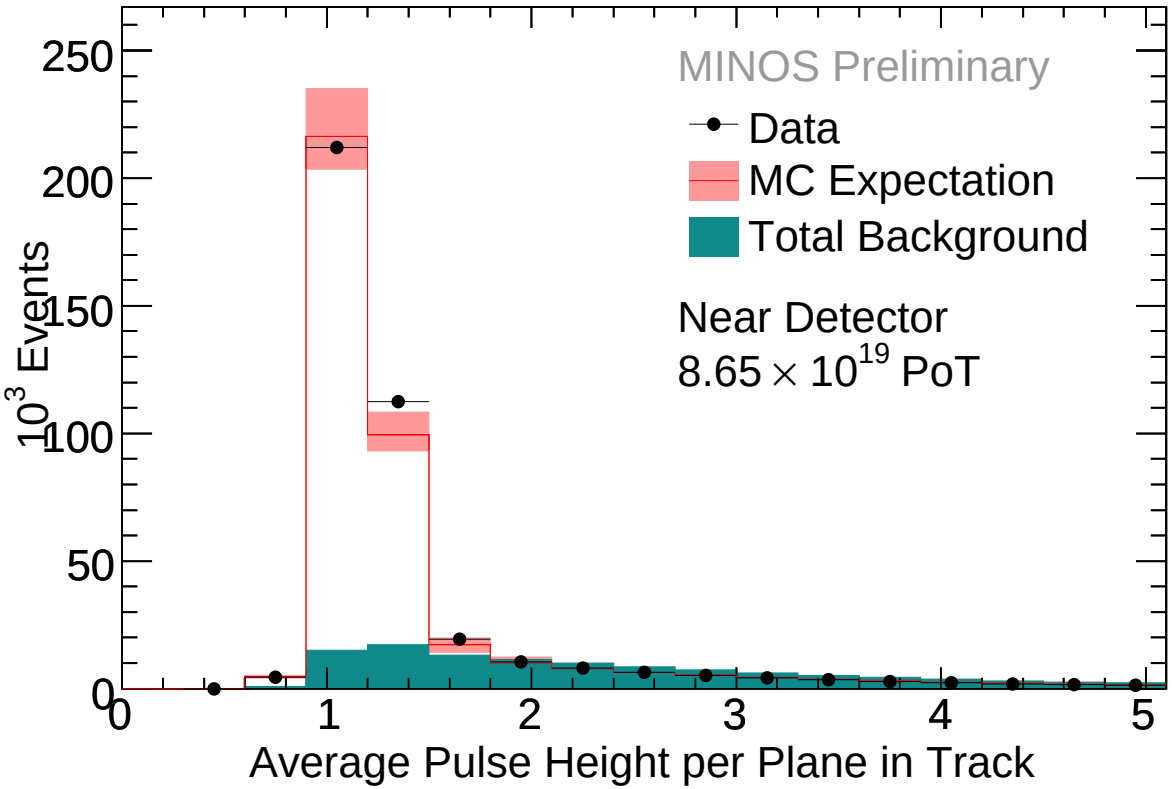

Figure 9: Distribution of PID input variable *mean pulse height in track* before the PID< 0.3 cut is applied. The red histogram represents the Monte Carlo expectation with the systematic error, the blue histogram represents the total (charged and neutral current) background with the background uncertaintiy. Black points represent data. minos-doc-7177

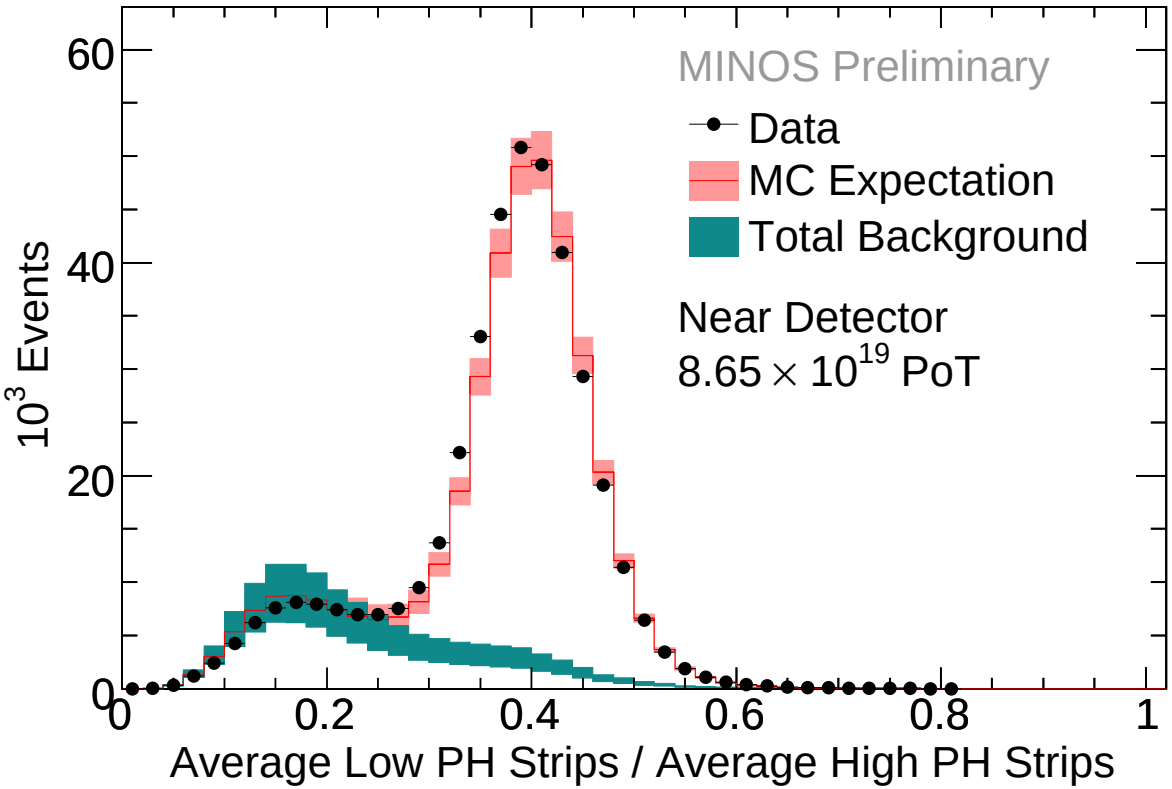

Figure 10: Distribution of PID input variable *ratio of mean low pulse height to mean high pulse height* before the PID< 0.3 cut is applied. The red histogram represents the Monte Carlo expectation with the systematic error, the blue histogram represents the total (charged and neutral current) background with the background uncertaintiy. Black points represent data. minos-doc-7177

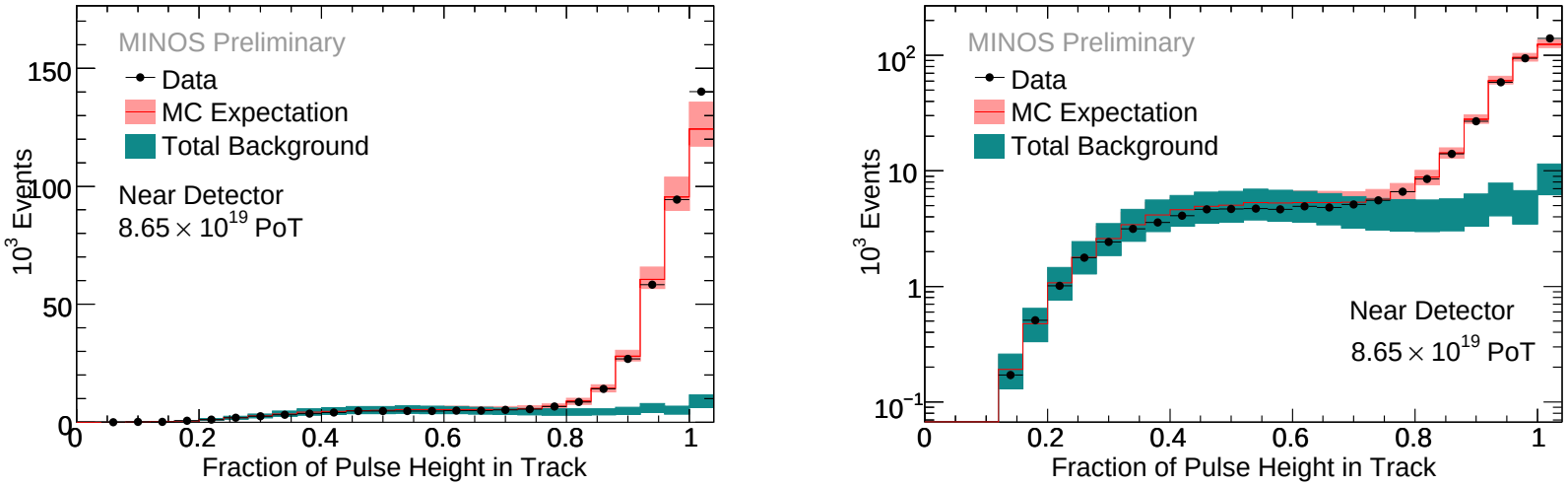

Figure 11: Distribution of PID input variable *transverse profile parameter* measuring the fraction of pulse height in the muon track before the PID< 0.3 cut is applied. The red histogram represents the Monte Carlo expectation with the systematic error, the blue histogram represents the total (charged and neutral current) background with the background uncertaintiy. Black points represent data. minos-doc-7177

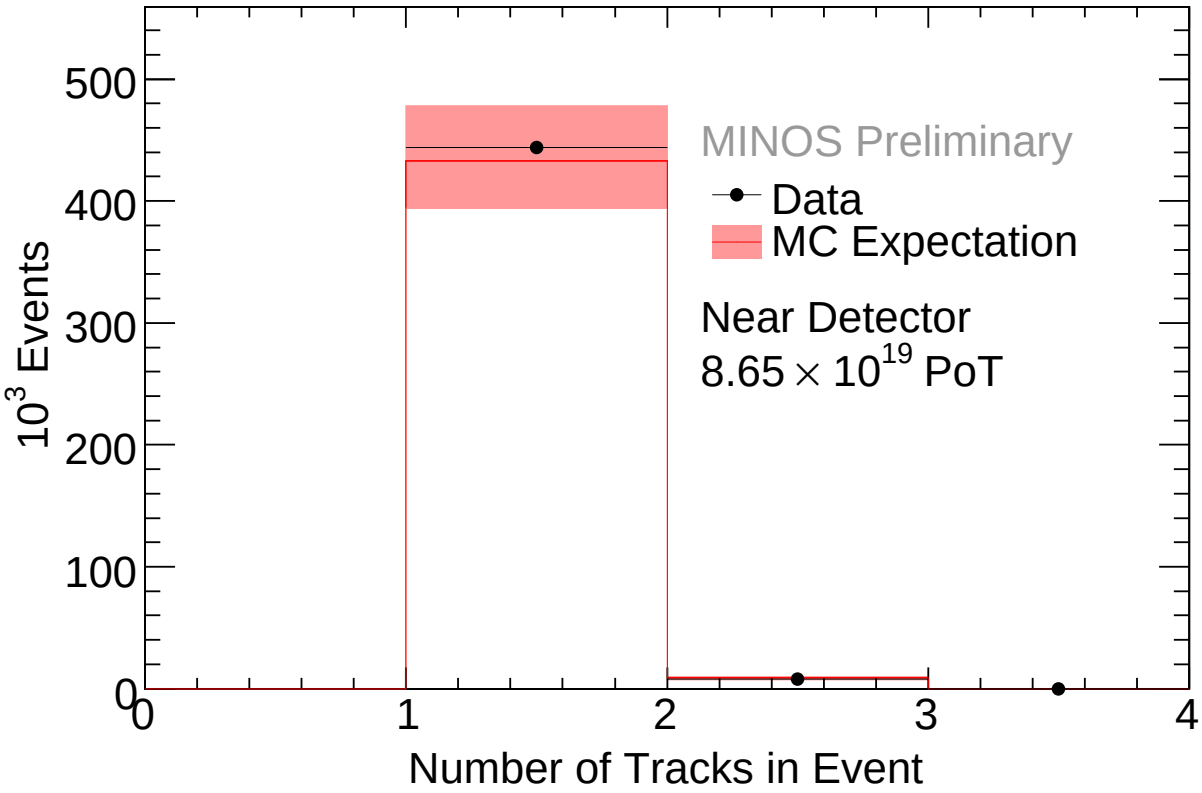

Figure 12: Number of tracks in selected charged current antineutrino interactions. The red histogram represents the Monte Carlo expectation with the systematic error and black points represent data. minos-doc-7177

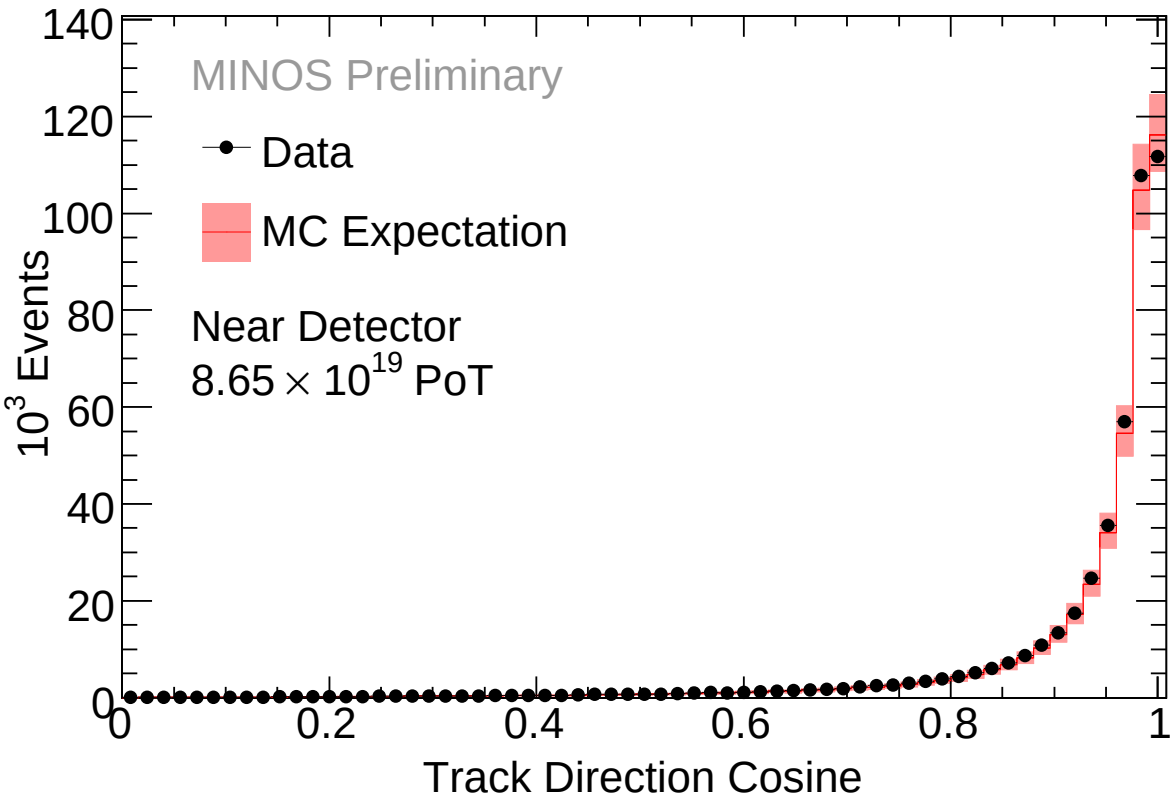

Figure 13: Cosine of the angle between the muon track and beam direction. The red histogram represents the Monte Carlo expectation with the systematic error and black points represent data. minos-doc-7177

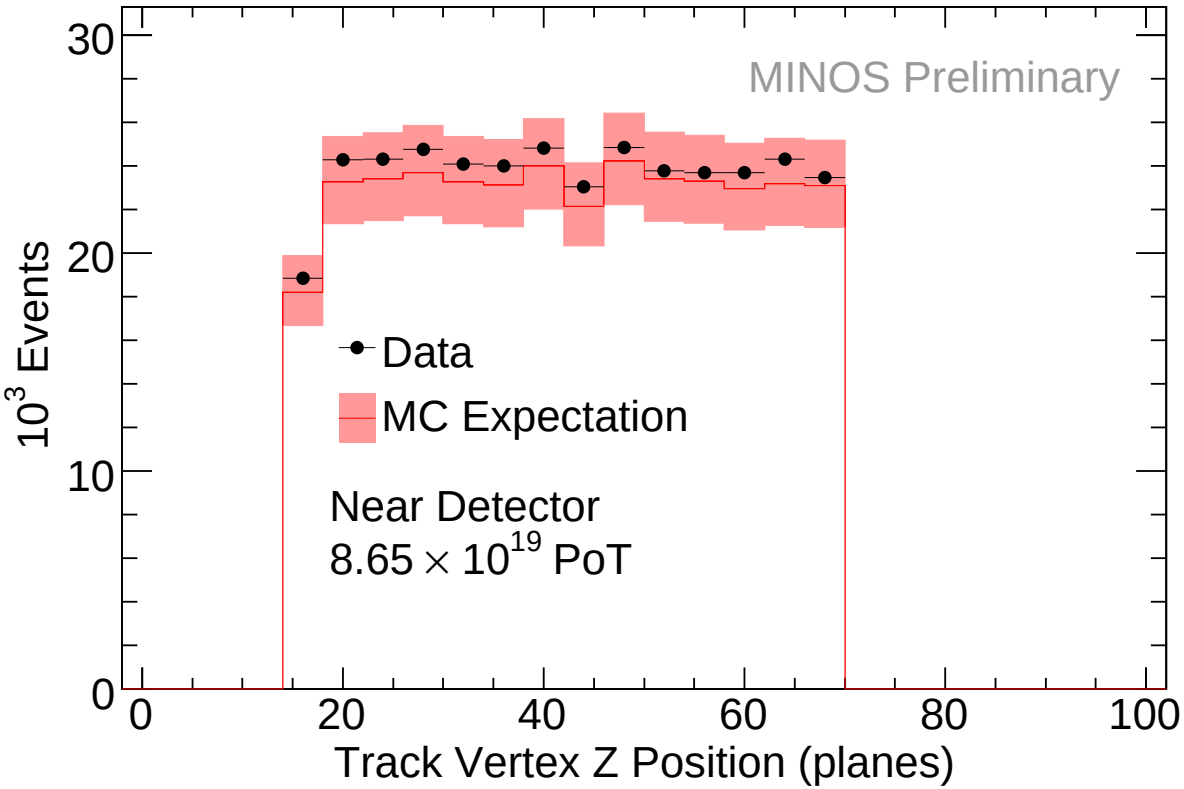

Figure 14: Near Detector track vertex longitudinal position distribution in planes. The red histogram represents the Monte Carlo expectation with the systematic error and black points represent data. minos-doc-7177

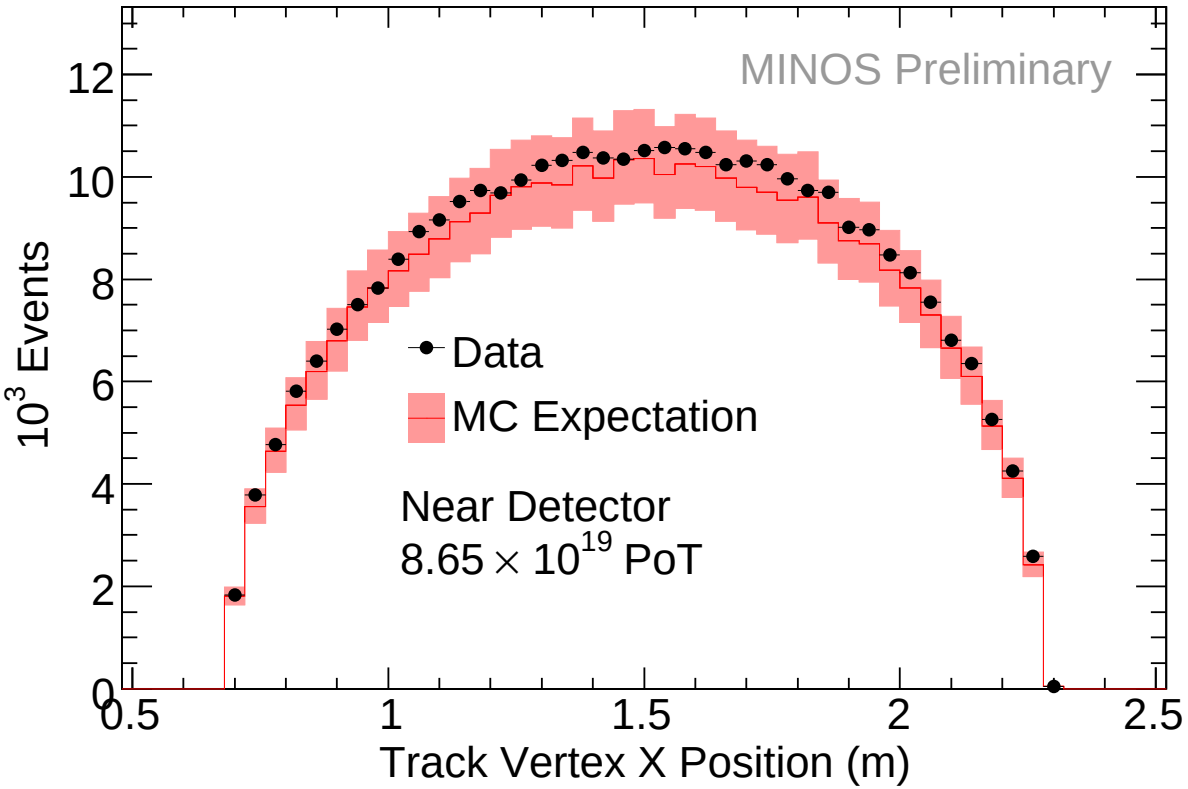

Figure 15: Near Detector track vertex X position distribution. The red histogram represents the Monte Carlo expectation with the systematic error and black points represent data. minos-doc-7177

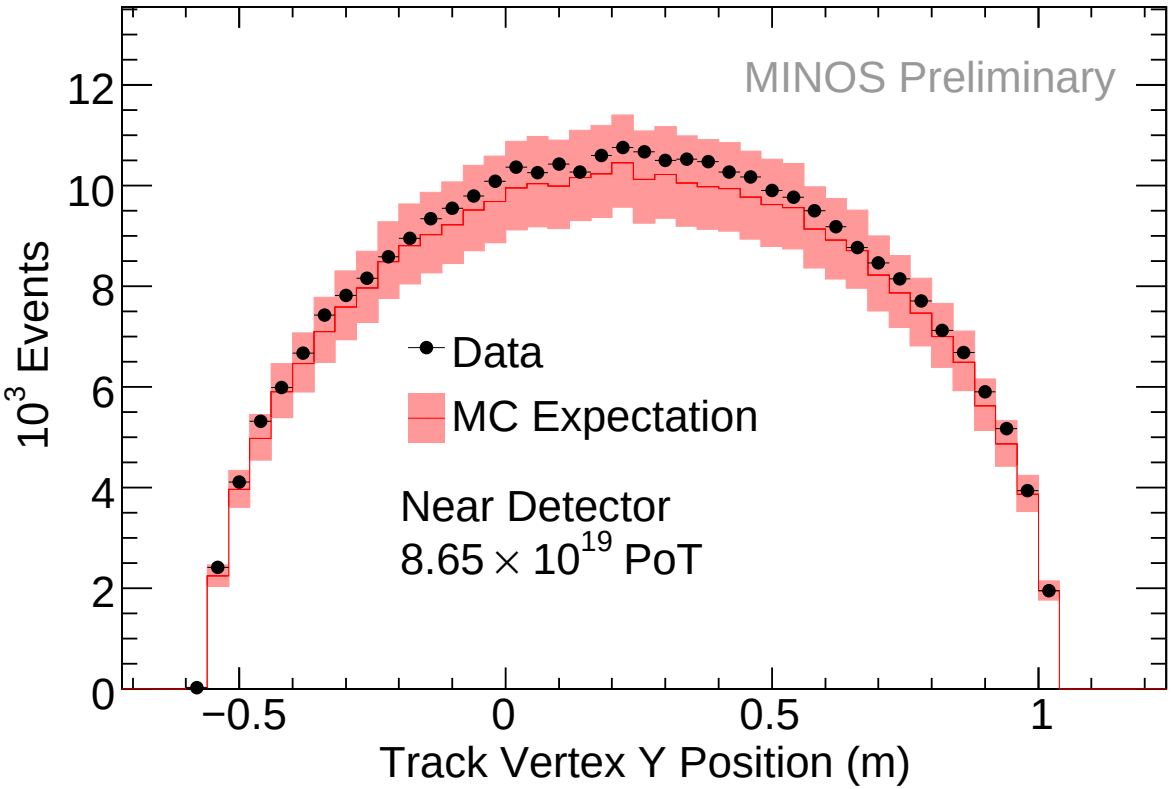

Figure 16: Near Detector track vertex Y position distribution. The red histogram represents the Monte Carlo expectation with the systematic error and black points represent data. minos-doc-7177

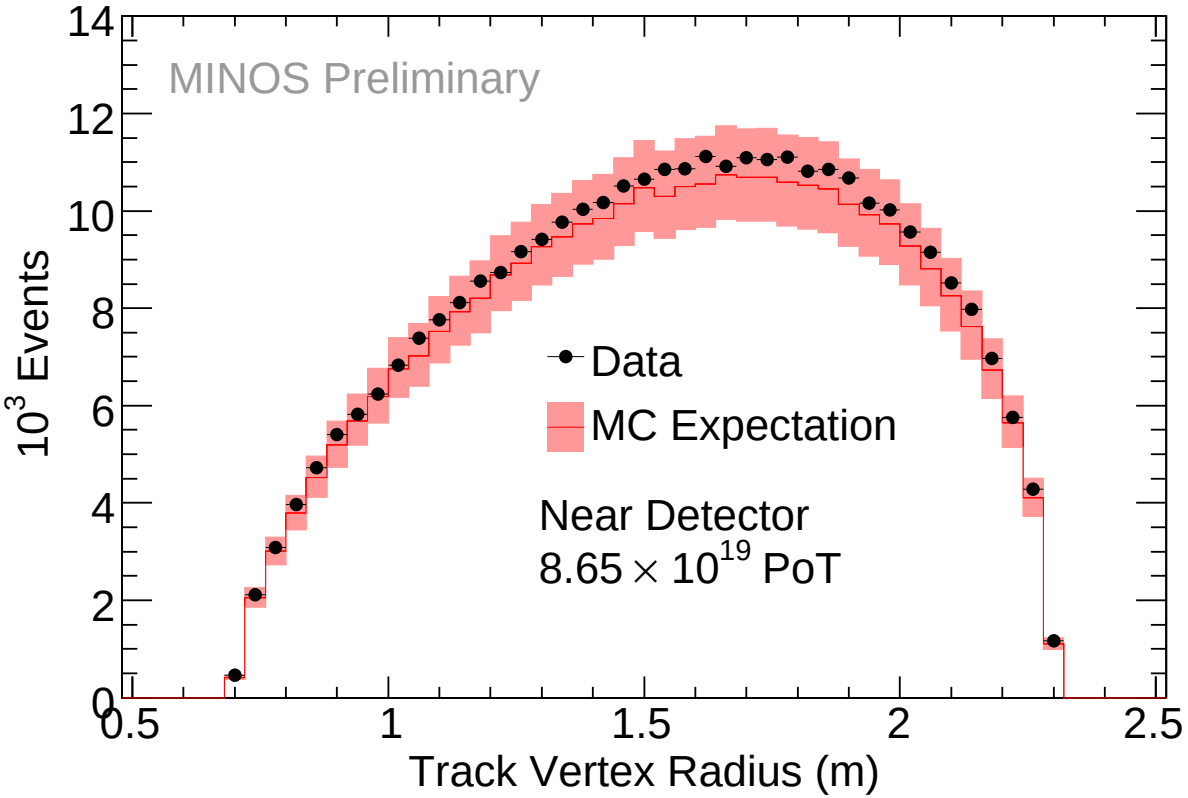

Figure 17: Near Detector track vertex radius distribution. The red histogram represents the Monte Carlo expectation with the systematic error and black points represent data. minos-doc-7177

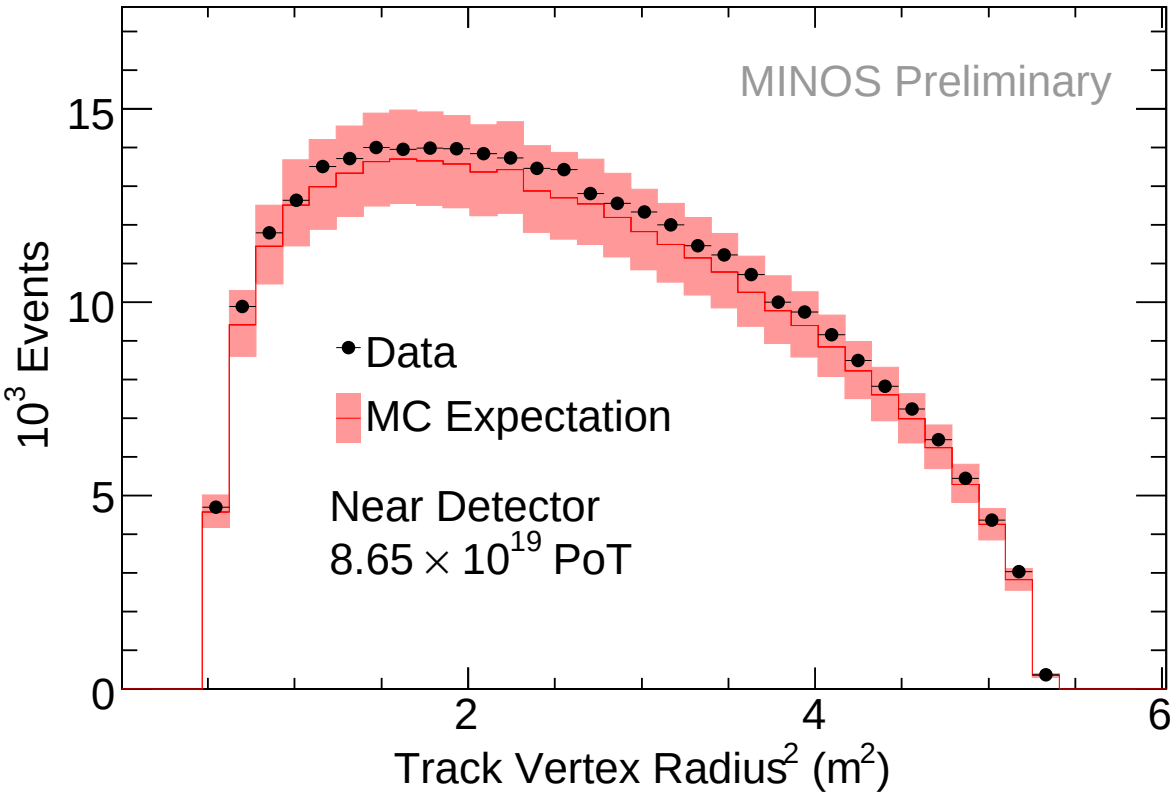

Figure 18: Near Detector track vertex radius^2 distribution. The red histogram represents the Monte Carlo expectation with the systematic error and black points represent data. minos-doc-7177

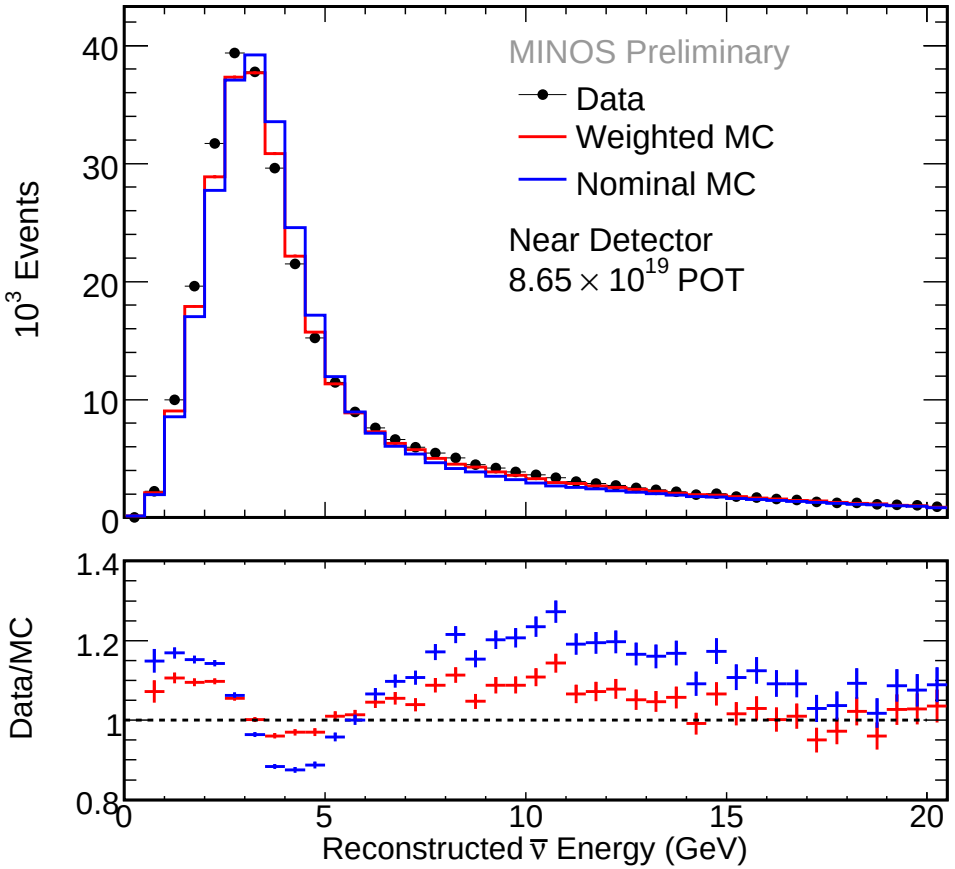

Figure 19: Nominal (unweighted) and flux weighted Monte Carlo reconstructed antineutrino energy distribution in the Near Detector compared to data. MC is PoT scaled to Data. minos-doc-7177

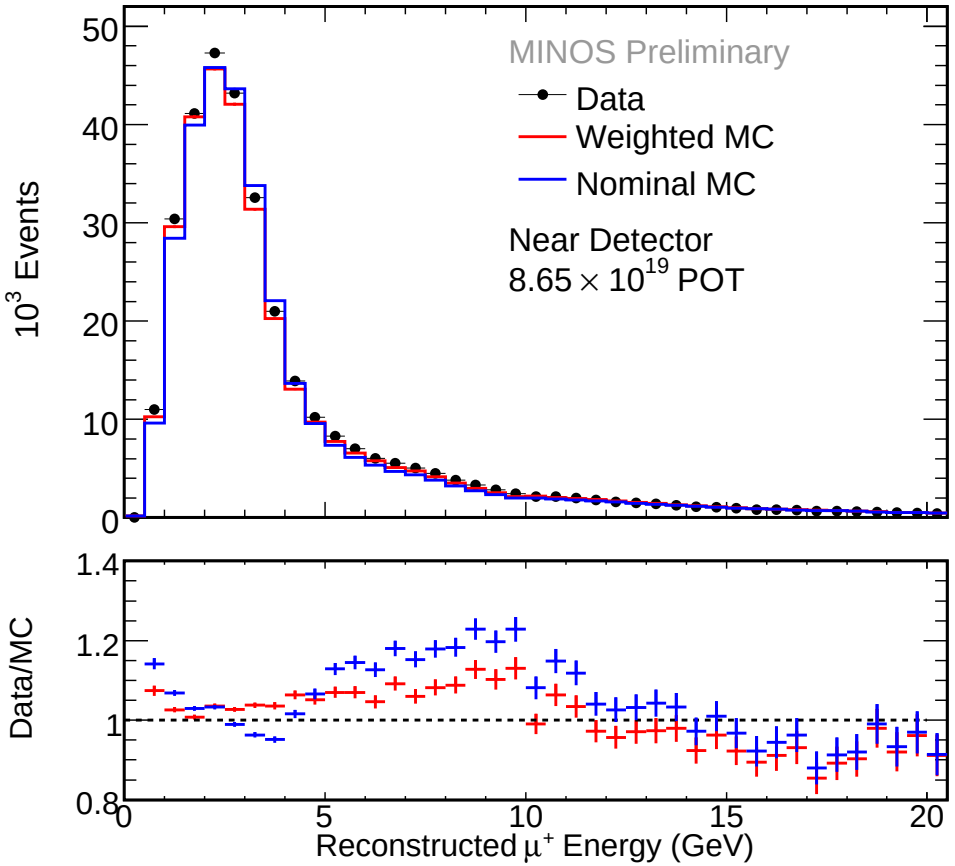

Figure 20: Nominal (unweighted) and flux weighted Monte Carlo reconstructed μ^+ momentum distribution in the Near Detector compared to data. MC is PoT scaled to Data. minos-doc-7177

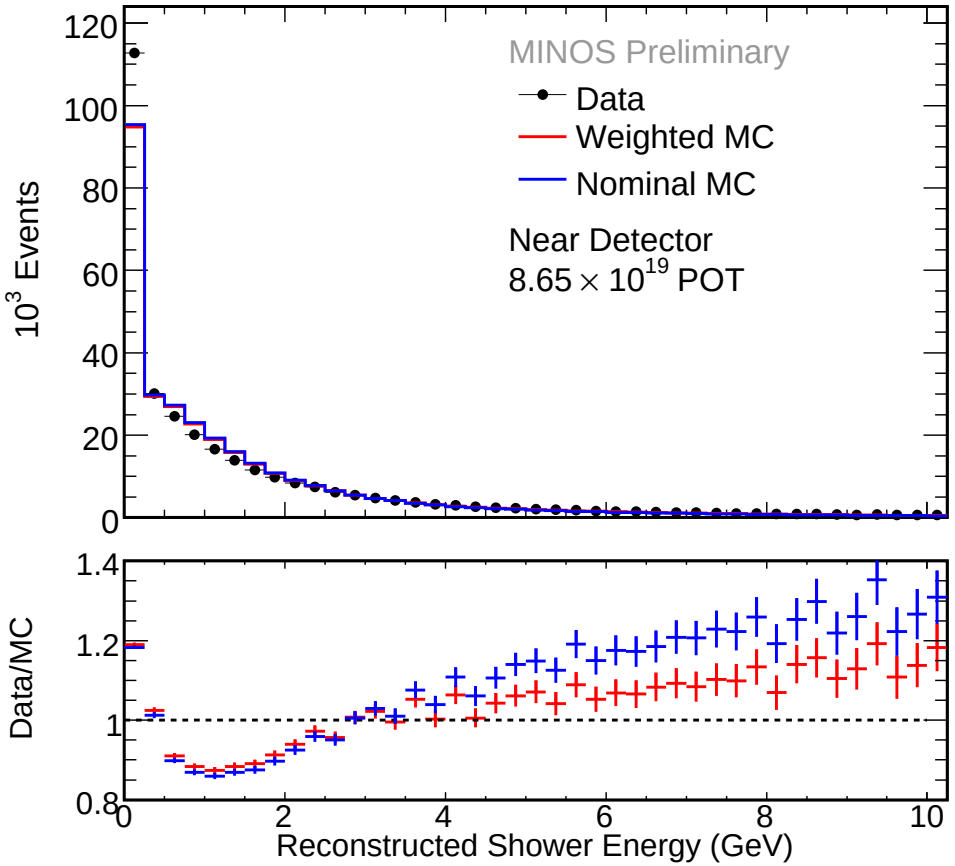

Figure 21: Nominal (unweighted) and flux weighted Monte Carlo reconstructed hadronic shower energy distribution in the Near Detector compared to data. MC is PoT scaled to Data. minos-doc-7177

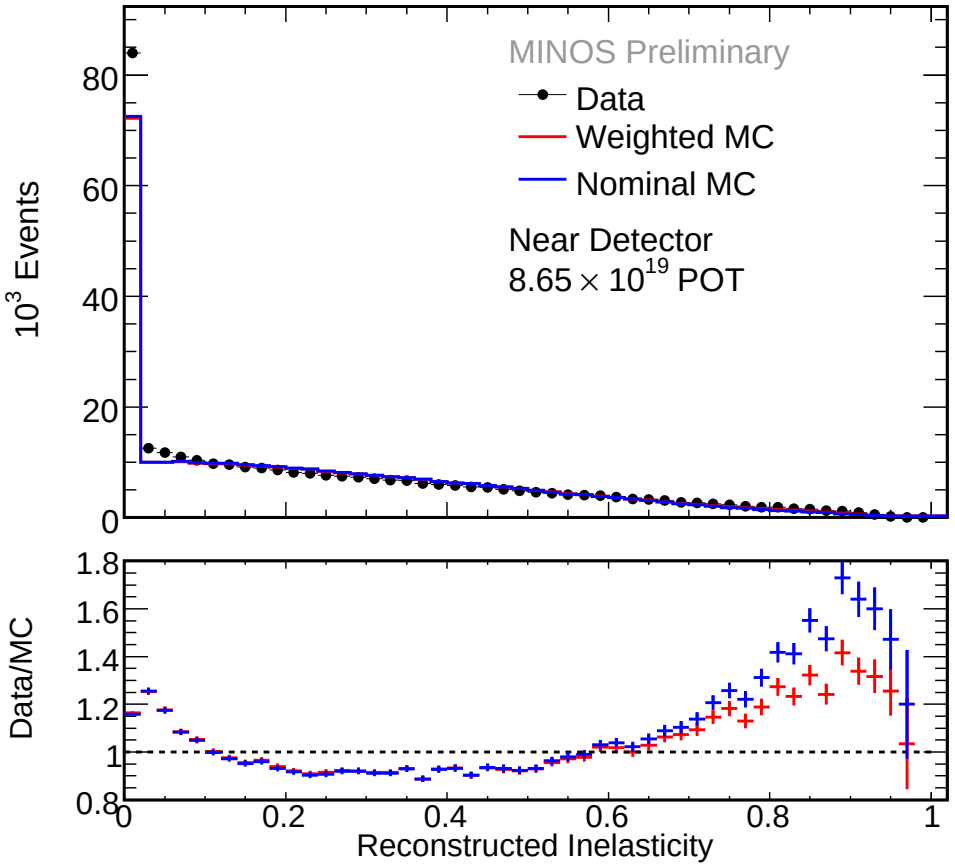

Figure 22: Nominal (unweighted) and flux weighted Monte Carlo reconstructed inelasticity distribution in the Near Detector compared to data. MC is PoT scaled to Data. minos-doc-7177

- Event times relative to the spill

ND Data Stability

minos-doc-7210

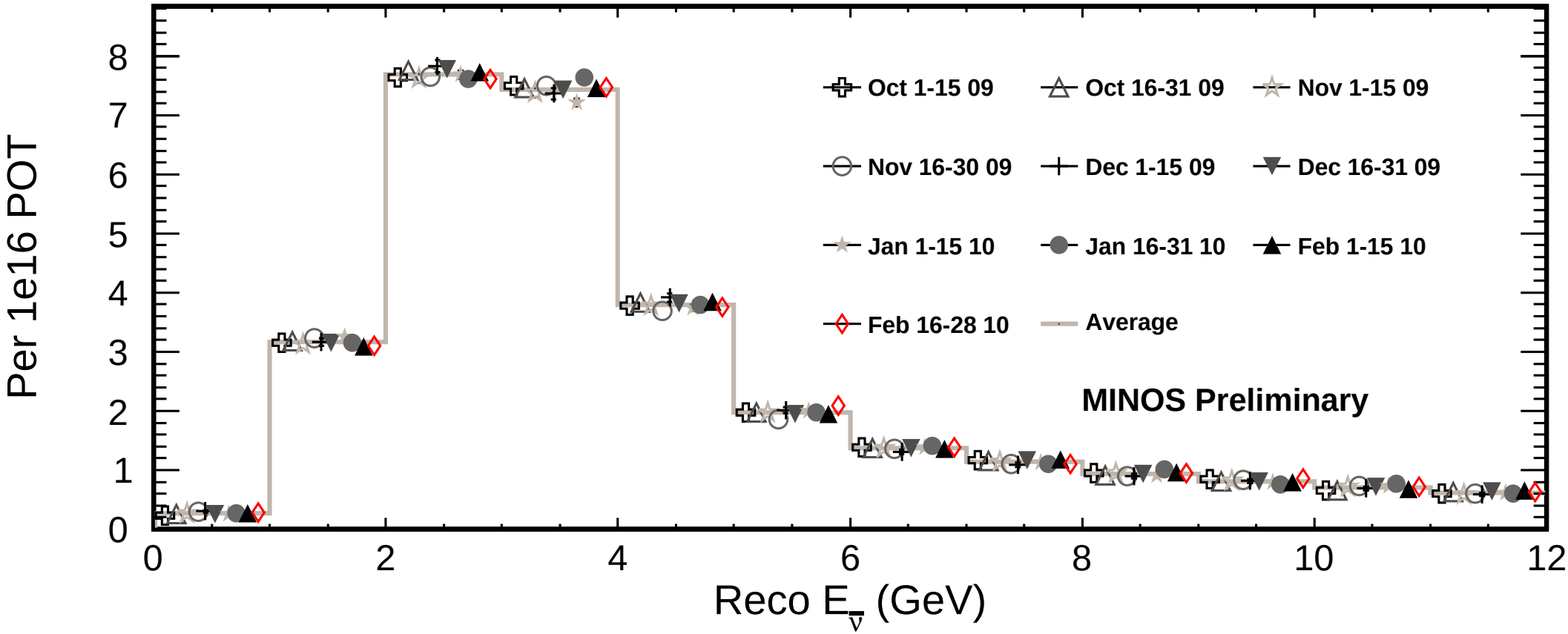

Figure 23: Energy Spectrum run IV broken up into time periods. Each individual time period is shown for bins of 1 GeV (normalized to POT). The average number of events in each bin is also shown. Visual inspection shows that for each bin the beam was stable for run IV. minos-doc-7210

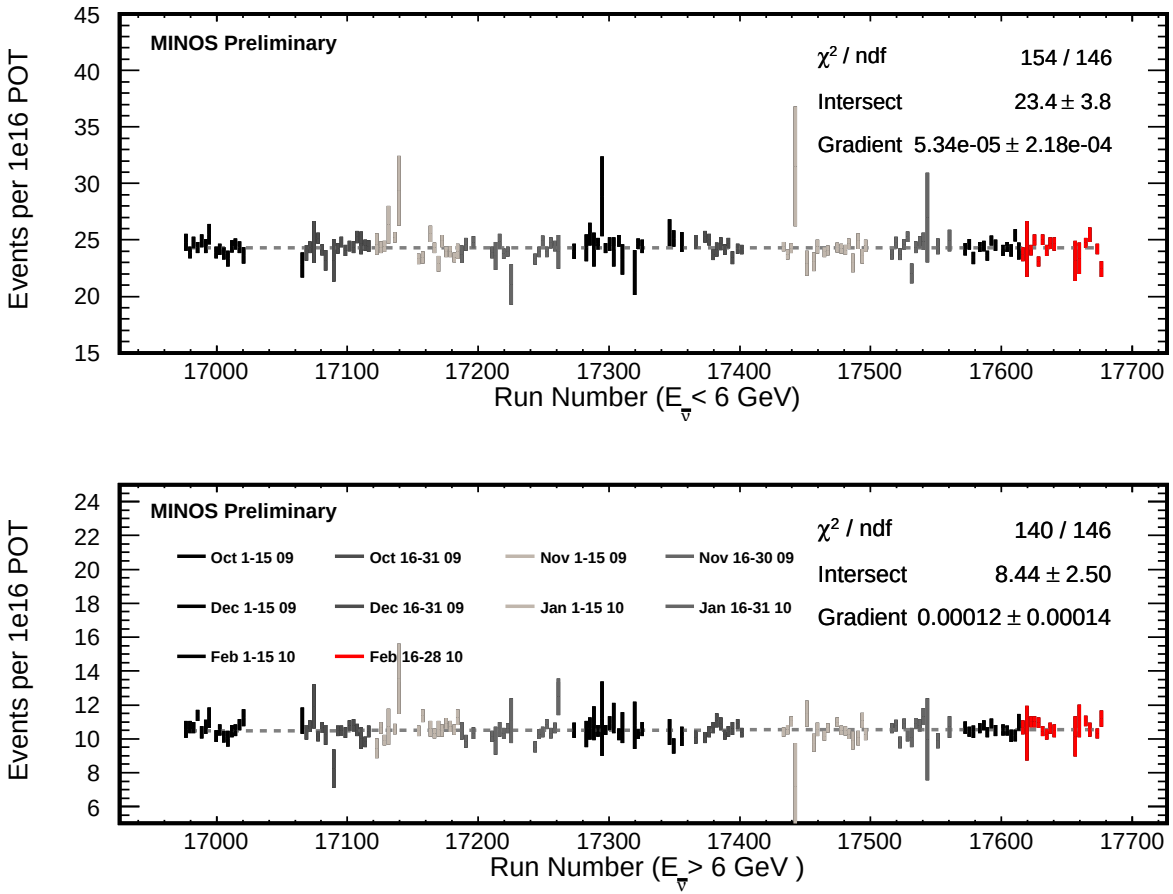

Figure 24: Run IV was divided up in to separate data sets: events in the beam peak and events in the high energy tail. Each data set was then fit to a line separately. The results of the fits are shown from which we can conclude that the beam was stable through out run IV. minos-doc-7210

FD Data/MC distributions

minos-doc-7030

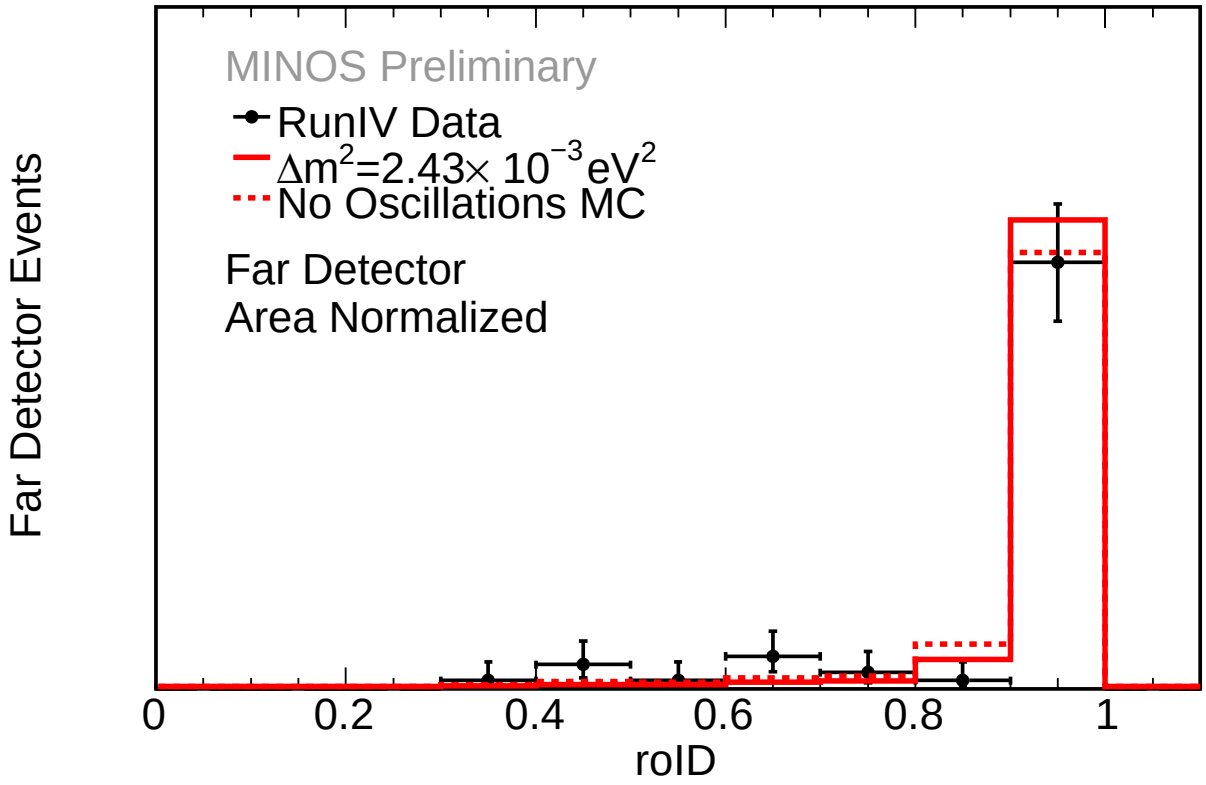

Figure 25: PID distribution of selected $\overline{\nu}_\mu$ events in the Far Detector. The solid red histogram represents the CPT conserving Monte Carlo expectation, the dashed red histogram represents the no oscillations expectation and black points represent data. MC is area nornalized to data and the y-axis is blinded to mask the appearance of oscillations. minos-doc-7030

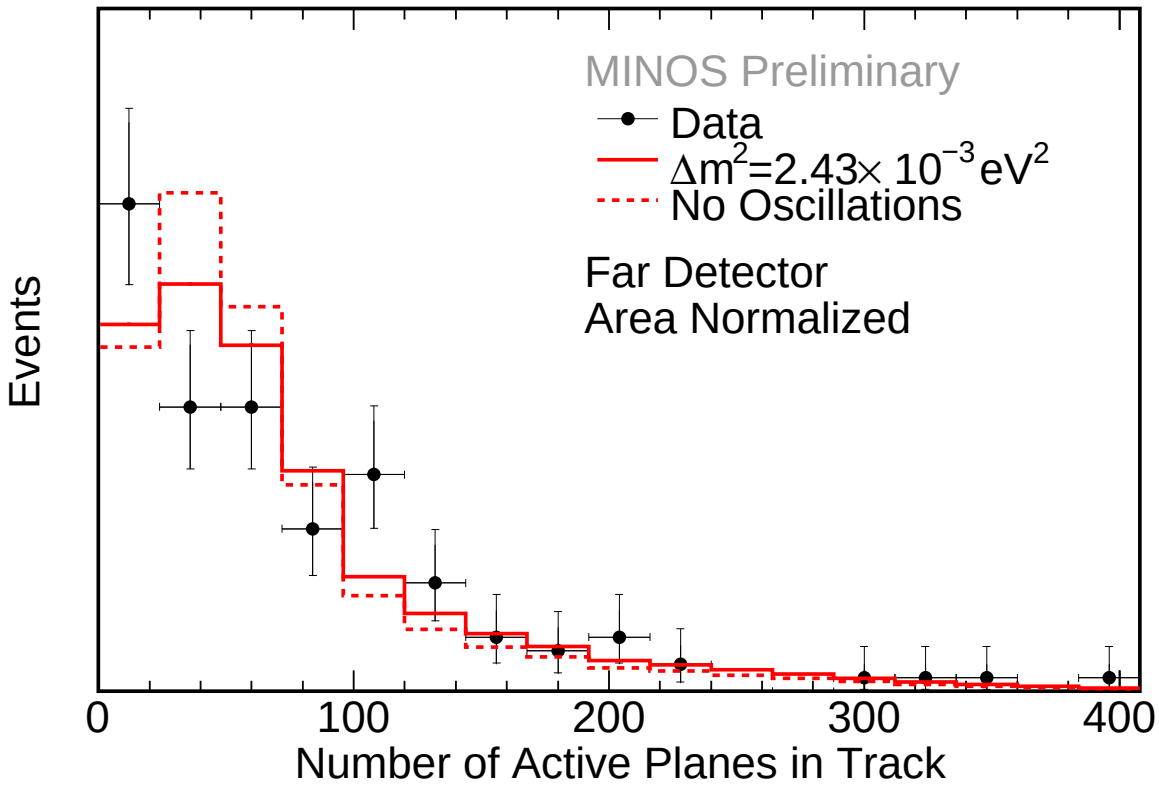

Figure 26: Distribution of PID input variable *number of active scintillator planes in track* before the PID< 0.3 cut is applied. The red histogram represents the Monte Carlo expectation with CPT conserving oscillations, the dashed red histogram represents the no oscillations case. Black points represent data. minos-doc-7030

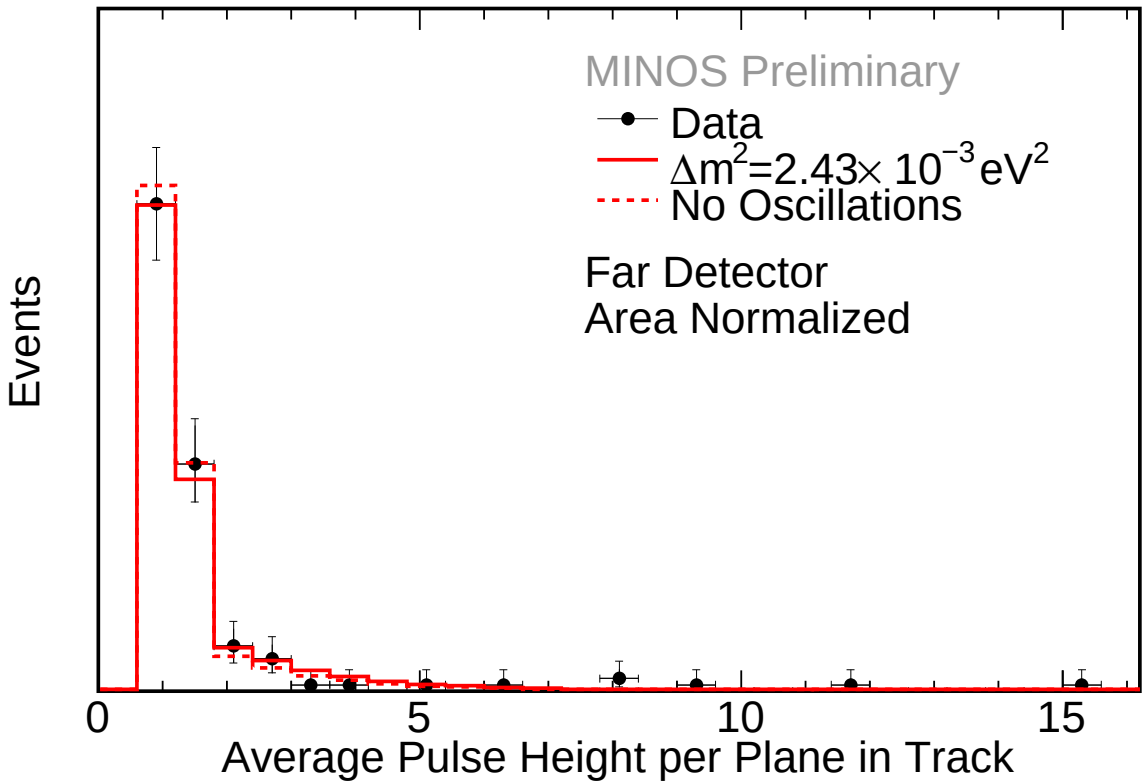

Figure 27: Distribution of PID input variable *mean pulse height in track* before the PID<0.3 cut is applied. The red histogram represents the Monte Carlo expectation with CPT conserving oscillations, the dashed red histogram represents the no oscillations case. Black points represent data. minos-doc-7030

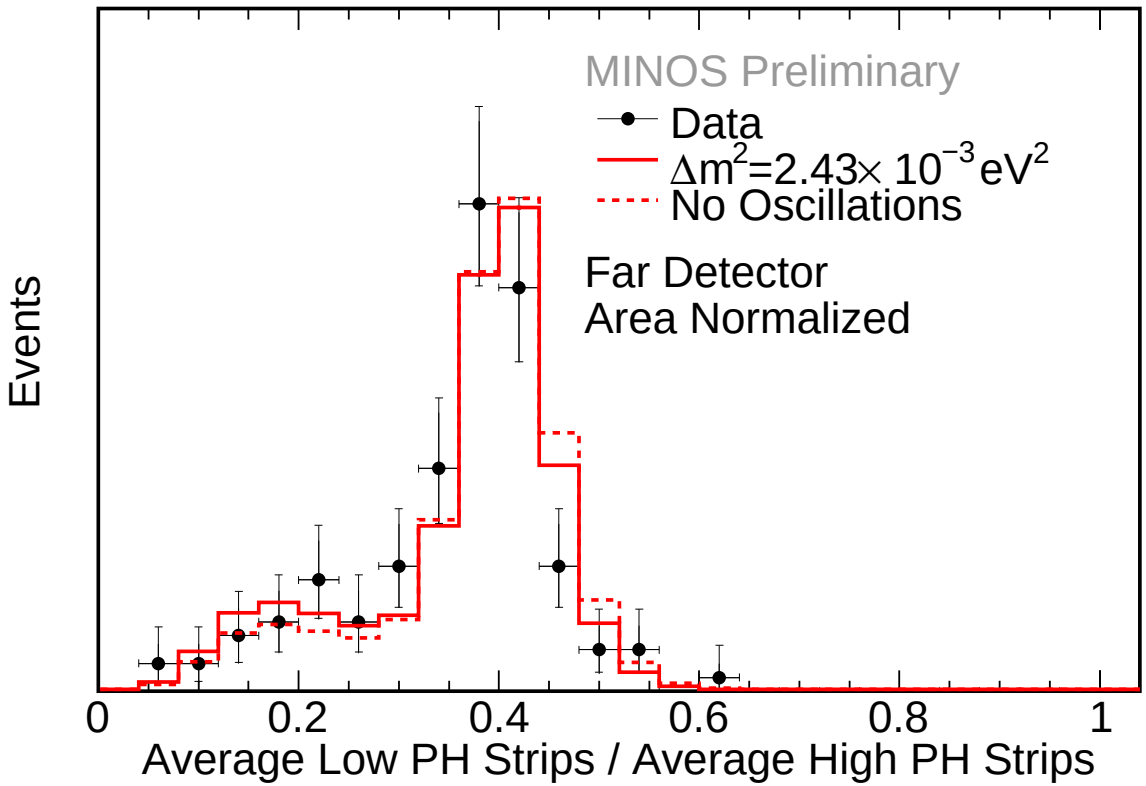

Figure 28: Distribution of PID input variable *ratio of mean low pulse height to mean high pulse height* before the PID< 0.3 cut is applied. The red histogram represents the Monte Carlo expectation with CPT conserving oscillations, the dashed red histogram represents the no oscillations case. Black points represent data. minos-doc-7030

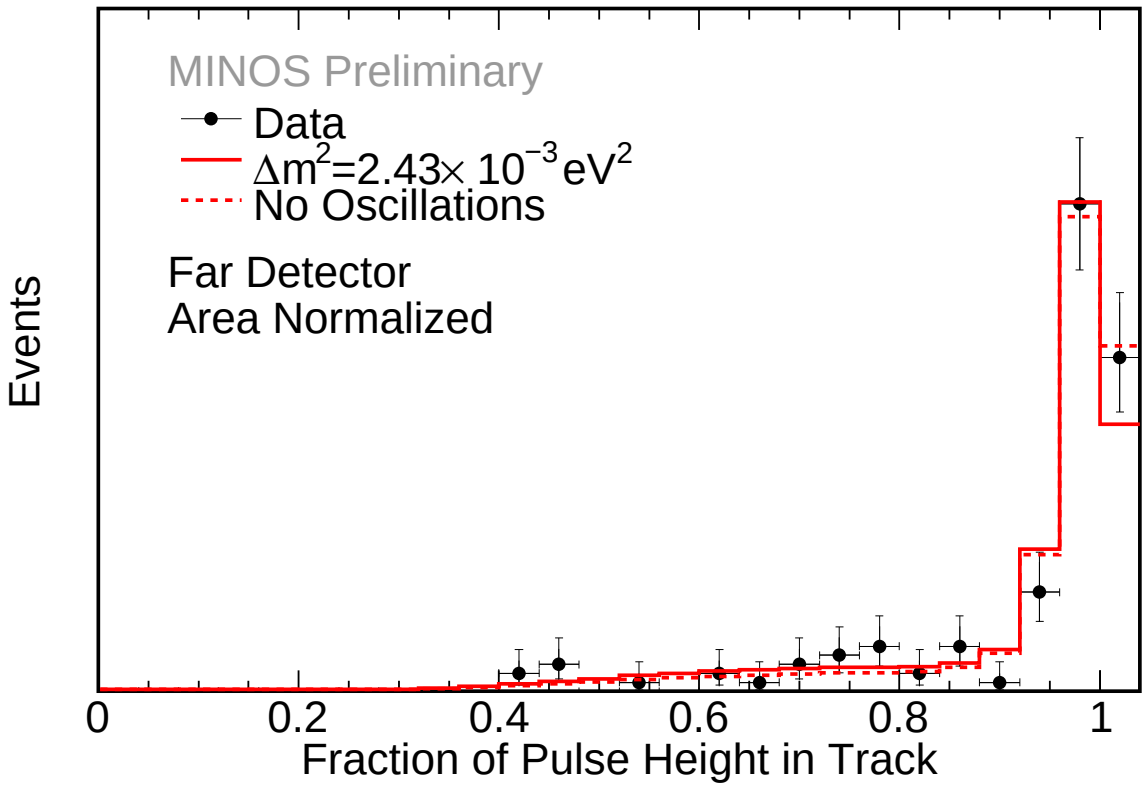

Figure 29: Distribution of PID input variable *transverse profile parameter* measuring the fraction of pulse height in the muon track before the PID< 0.3 cut is applied. The red histogram represents the Monte Carlo expectation with CPT conserving oscillations, the dashed red histogram represents the no oscillations case. Black points represent data. minos-doc-7030

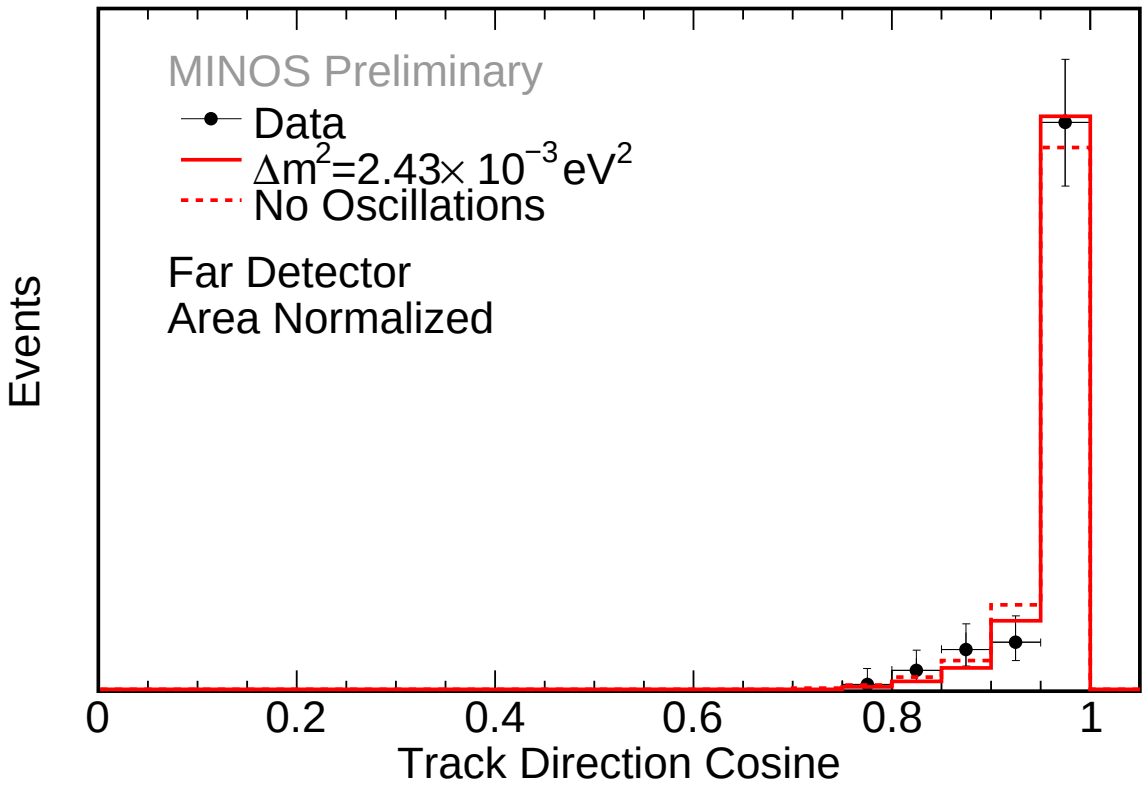

Figure 30: Cosine of the angle between the muon track and beam direction in the Far Detector. Preselection refuses $\theta < 0.6$ to reduce background from cosmic rays. The solid red histogram represents the CPT conserving Monte Carlo expectation, the dashed red histogram represents the no oscillations expectation and black points represent data. MC is area nornalized to data and the y-axis is blinded to mask the appearance of oscillations. minos-doc-7030

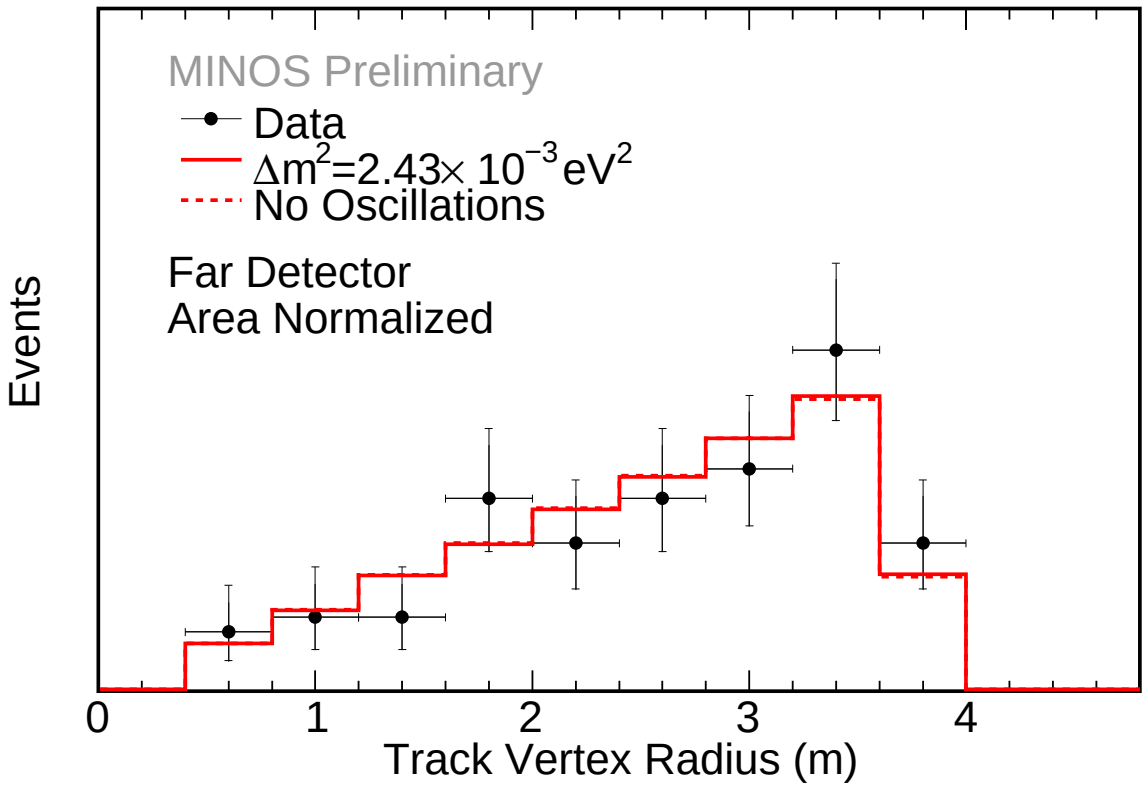

Figure 31: Track vertex radius distribution of selected $\overline{\nu}_\mu$ events in the Far Detector. The solid red histogram represents the CPT conserving Monte Carlo expectation, the dashed red histogram represents the no oscillations expectation and black points represent data. MC is area nornalized to data and the y-axis is blinded to mask the appearance of oscillations. minos-doc-7030

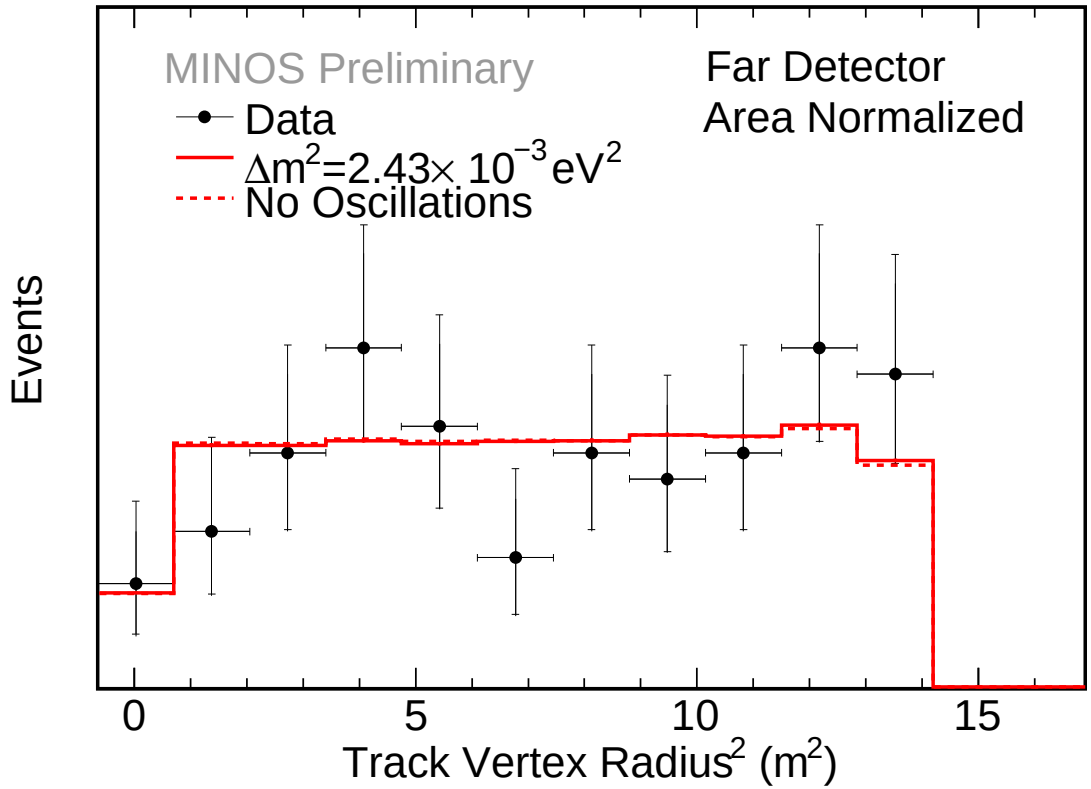

Figure 32: Track vertex radius^2 distribution of selected $\overline{\nu}_\mu$ events in the Far Detector. The solid red histogram represents the CPT conserving Monte Carlo expectation, the dashed red histogram represents the no oscillations expectation and black points represent data. MC is area nornalized to data and the y-axis is blinded to mask the appearance of oscillations. minos-doc-7030

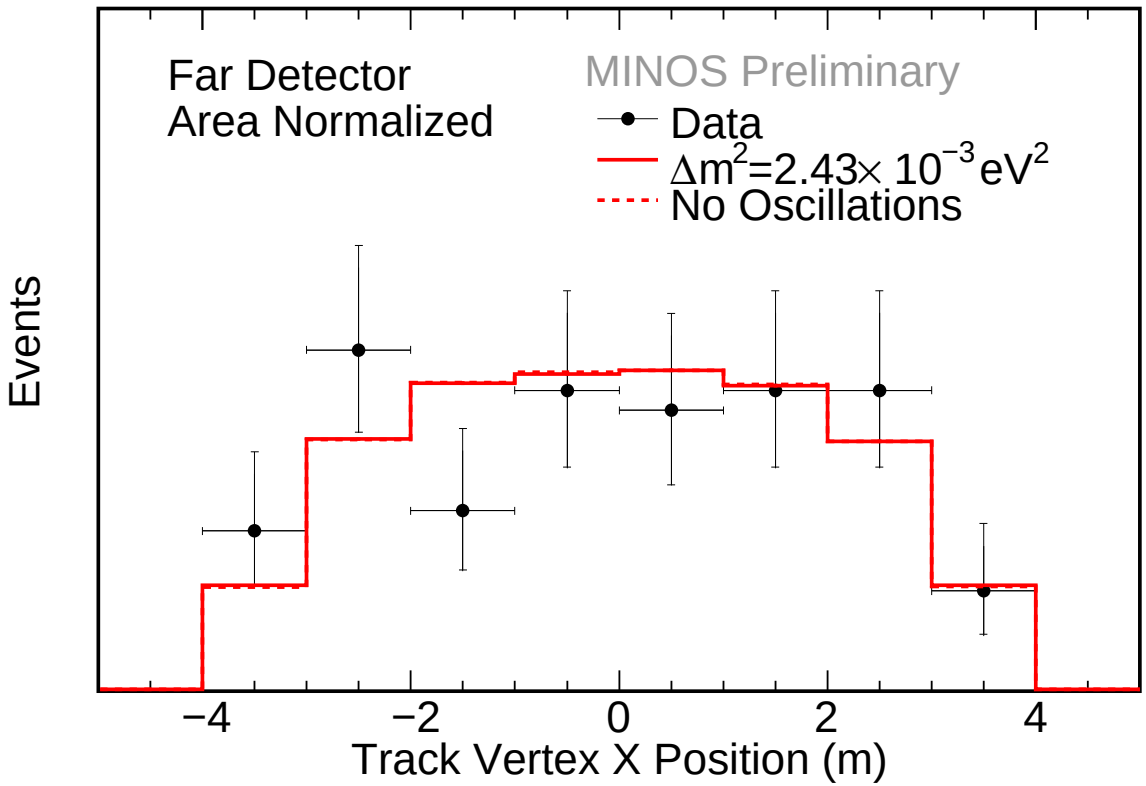

Figure 33: Track vertex X position distribution of selected $\overline{\nu}_\mu$ events in the Far Detector. The solid red histogram represents the CPT conserving Monte Carlo expectation, the dashed red histogram represents the no oscillations expectation and black points represent data. MC is area nornalized to data and the y-axis is blinded to mask the appearance of oscillations. minos-doc-7030

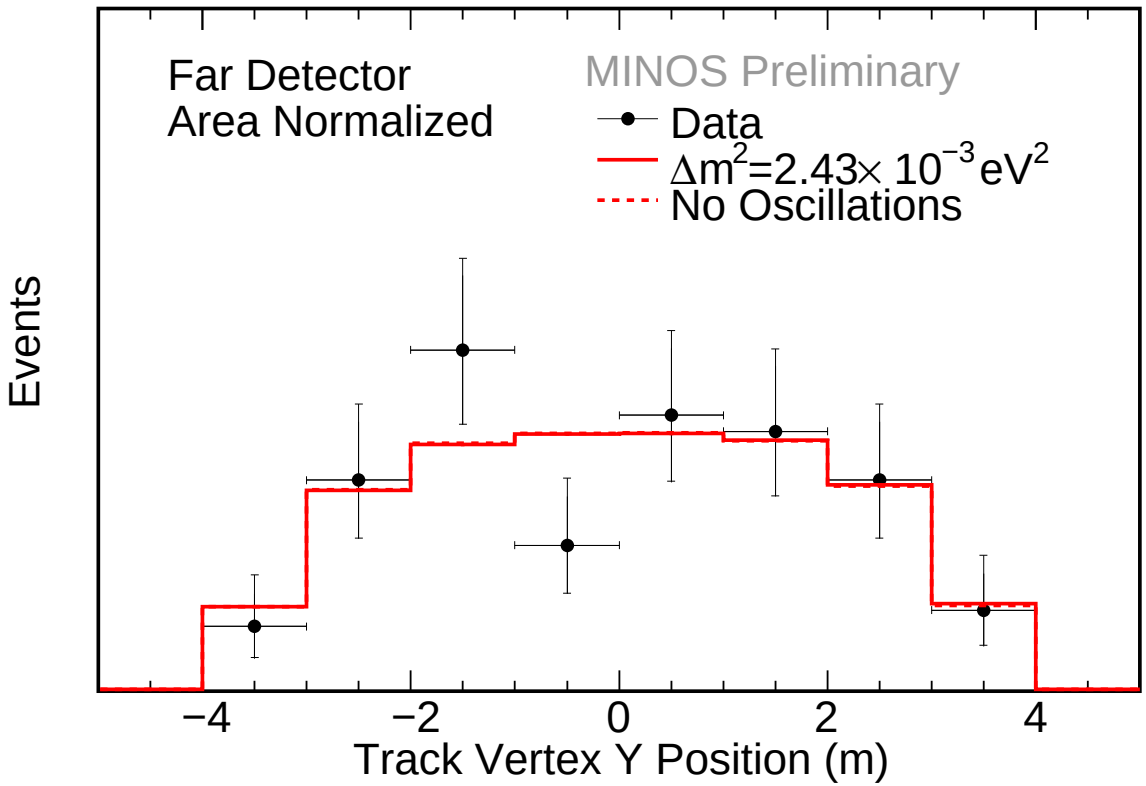

Figure 34: Track vertex Y position distribution of selected $\overline{\nu}_\mu$ events in the Far Detector. The solid red histogram represents the CPT conserving Monte Carlo expectation, the dashed red histogram represents the no oscillations expectation and black points represent data. MC is area nornalized to data and the y-axis is blinded to mask the appearance of oscillations. minos-doc-7030

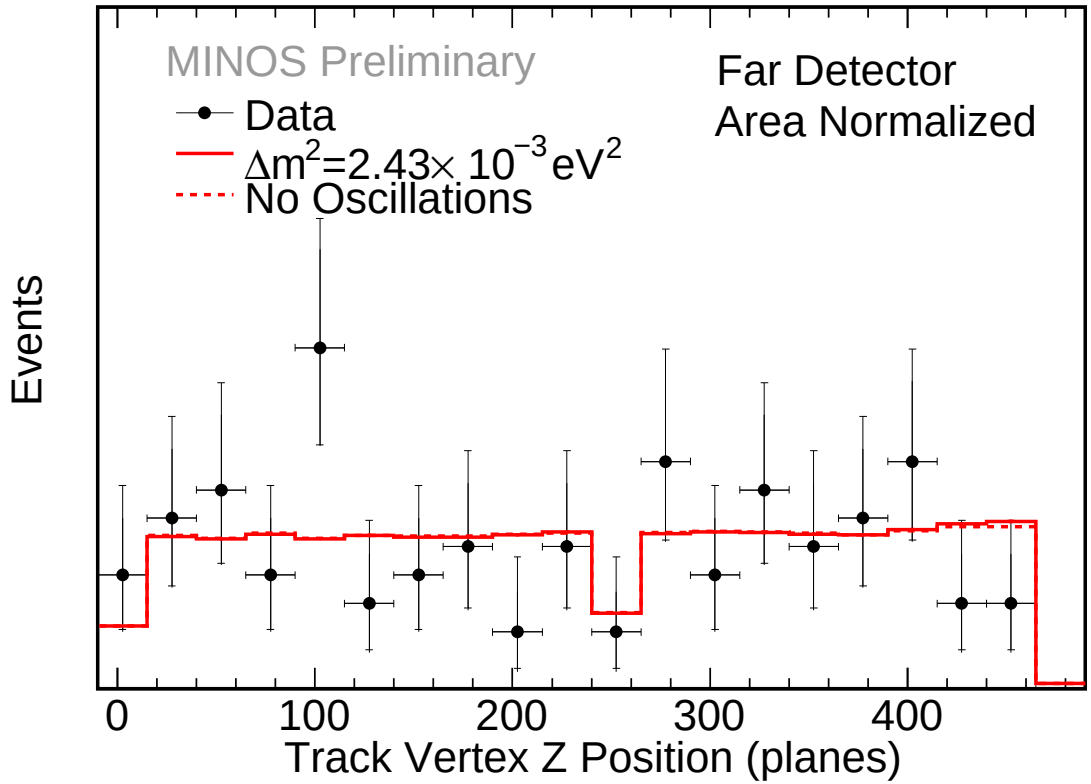

Figure 35: Track vertex longitudinal position distribution of selected $\overline{\nu}_\mu$ events in the Far Detector. The solid red histogram represents the CPT conserving Monte Carlo expectation, the dashed red histogram represents the no oscillations expectation and black points represent data. MC is area nornalized to data and the y-axis is blinded to mask the appearance of oscillations. minos-doc-7030

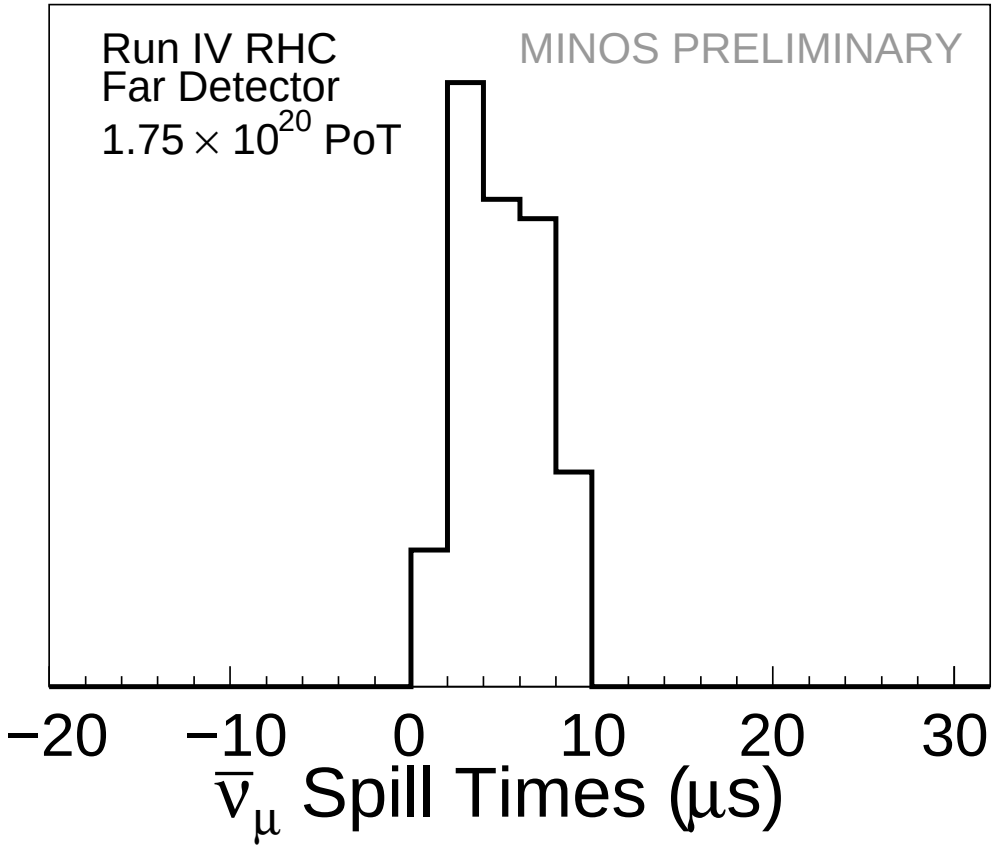

Figure 36: The relative time between the events and the beginning of the spill in the far detector data. The y-axis is blinded to mask the appearance of oscillations.minos-doc-7030

Coming after the box opening:

- Energy spectrum (MC to have SKZP flux weights only)
- Track energy spectrum
- Shower energy spectrum
- Number of tracks
- Reconstructed y
- Scatter plot of trackEndX v trackEndY
- Scatter plot of trackVtxX v trackVtxY

Extrapolation, Sensitivity, and Systematics

minos-doc-7136

minos-doc-7195

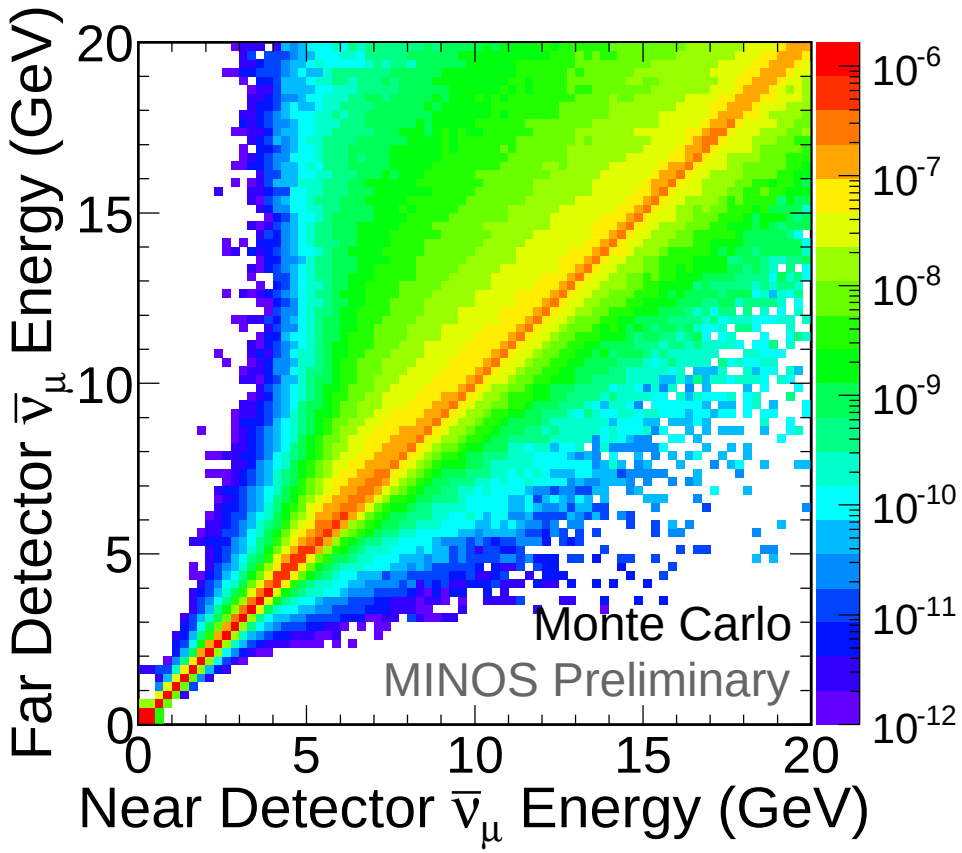

Figure 37: The beam matrix for numubar. The contents of each cell represent the mean number of numubar events expected in the Far detector for one event in the Near detector. This distribution is treated as a matrix to relate the energy measured in the ND to those in the FD. minos-doc-7136

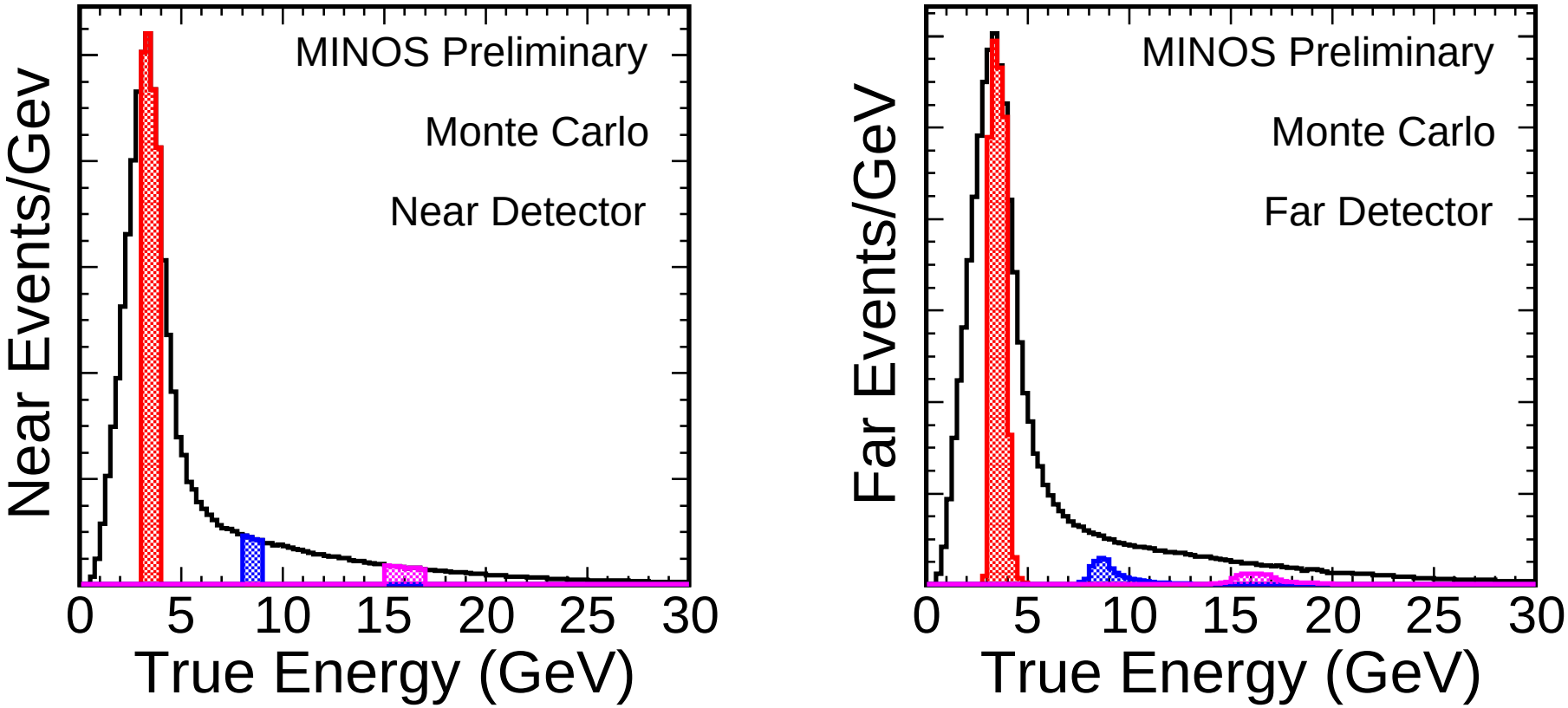

Figure 38: The relationship between the energy of numubar events observed in the near detector with those observed in the far detector. Decays of pi/K/mu producing events of a given energy in the near detector would produce a range of energies in the far detector, yielding the energy smearing seen here. This is the information encoded in the beam matrix. minos-doc-7136

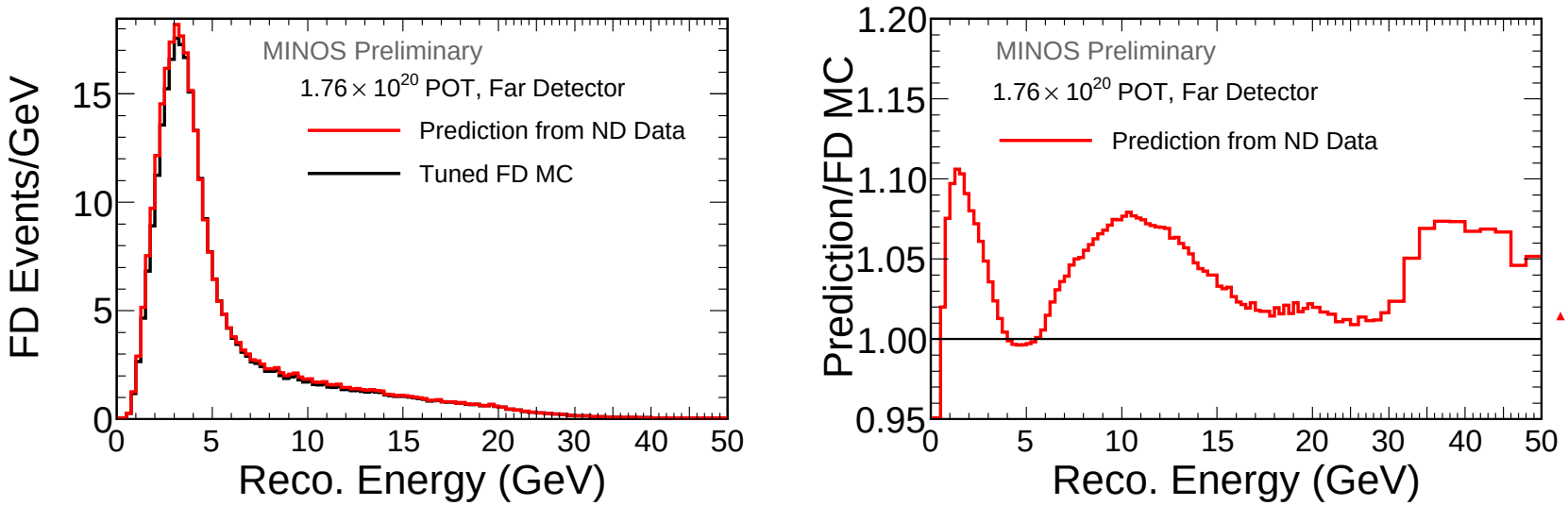

Figure 39: At left is the far detector prediction based on the near detector data (shown in red) compared with the far detector monte carlo (shown in black). At right is the ratio of prediction to monte carlo. minos-doc-7136

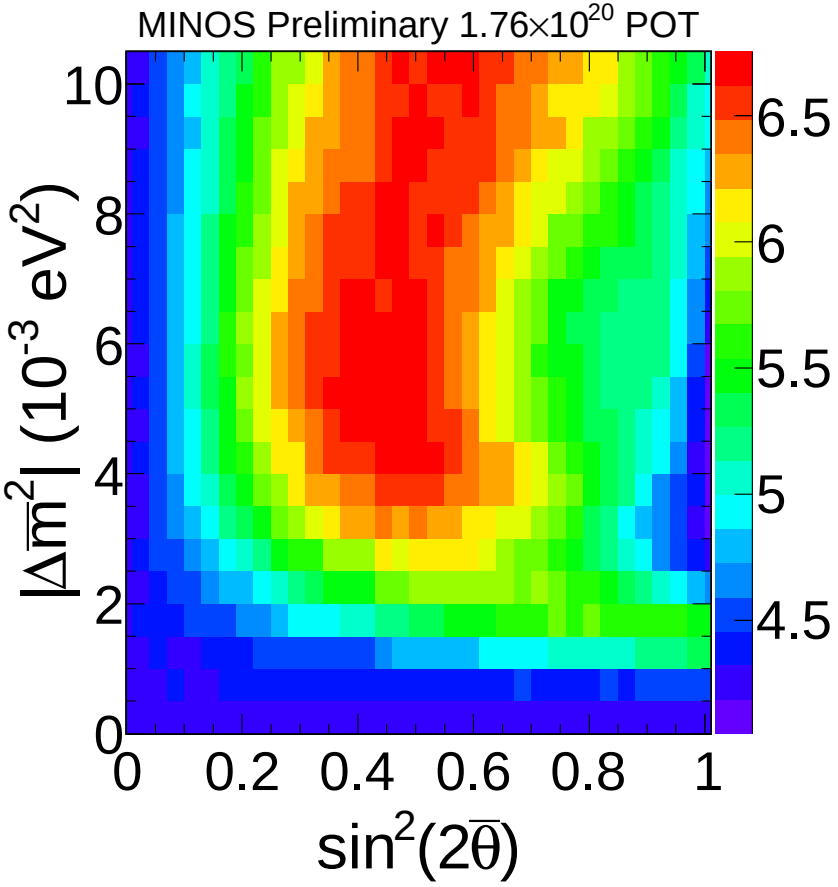

Figure 40: The 90% confidence level Feldman-Cousins grid for an RHC exposure of 1.76×10^{20} POT. The gaussian up-value for this confidence is 4.61, which is a medium-blue color. Values lower than this indicate areas where the contour is narrower than the gaussian expectation and vice-versa. The large rise around $\sin^2(2\bar{\theta}) = 0.5$ arises from an ambiguity between fast oscillations coming from high $\Delta\bar{m}^2$ and the true oscillations which both lower the focusing peak by about half. minos-doc-7136

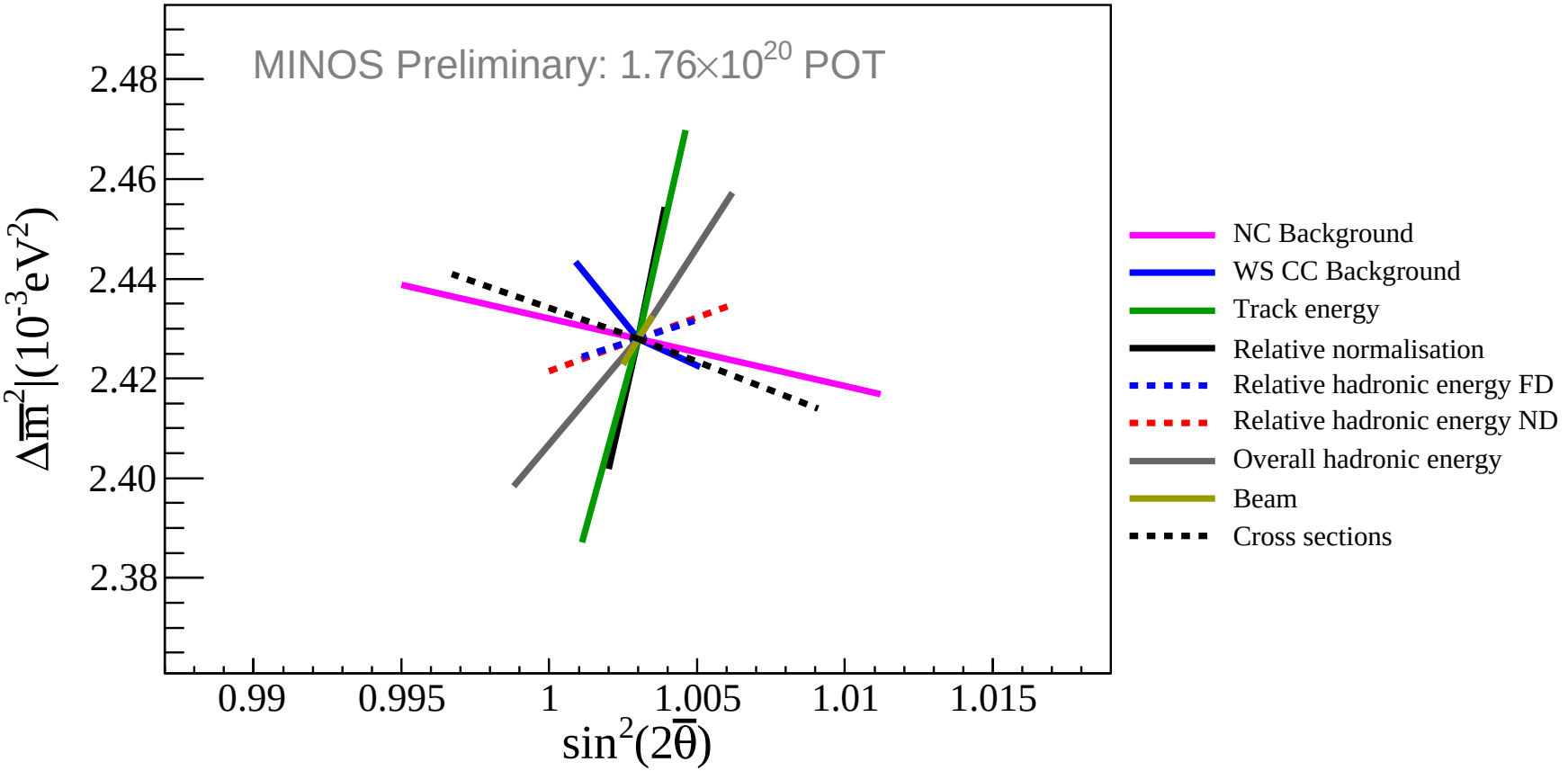

Figure 41: The shifts to the best fit oscillation parameters induced by the application of the 2010 NuMuBar RHC analysis systematic shifts to the fake data. The sum, in quadrature, of all cross section shifts is also shown. minos-doc-7195

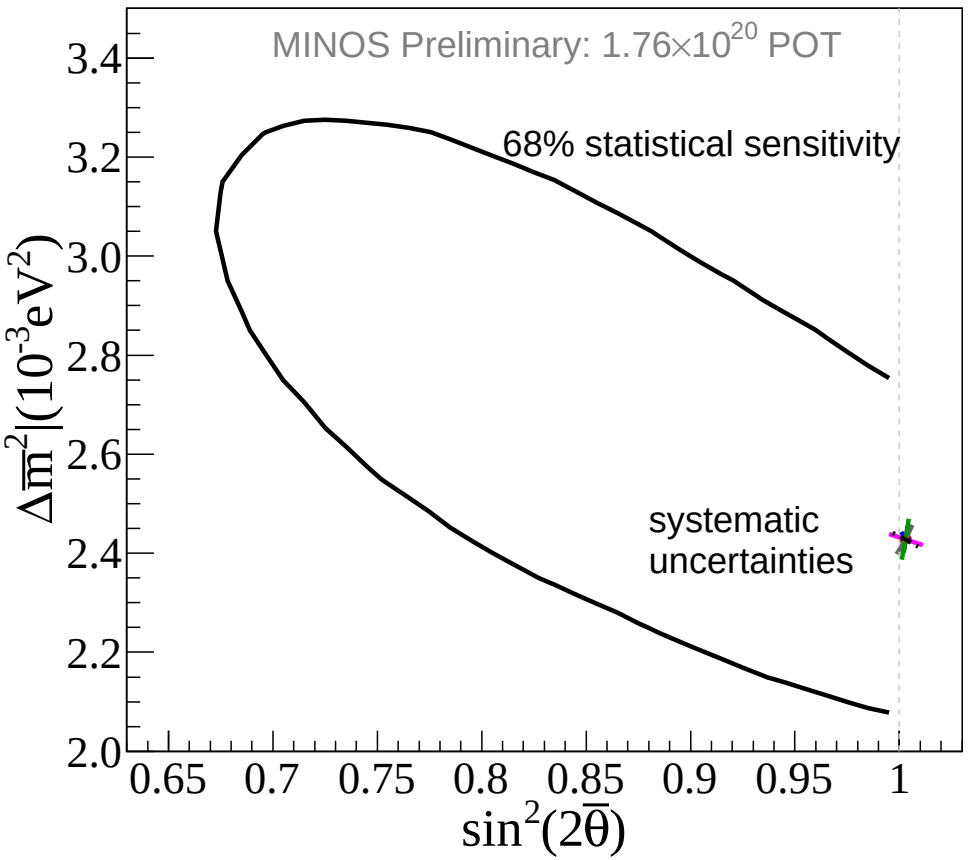

Figure 42: The shifts to the best fit oscillation parameters and the statistical sensitivity contour (black curve). minos-doc-7195

Systematics Error Band

Oscillation Results

minos-doc-7204

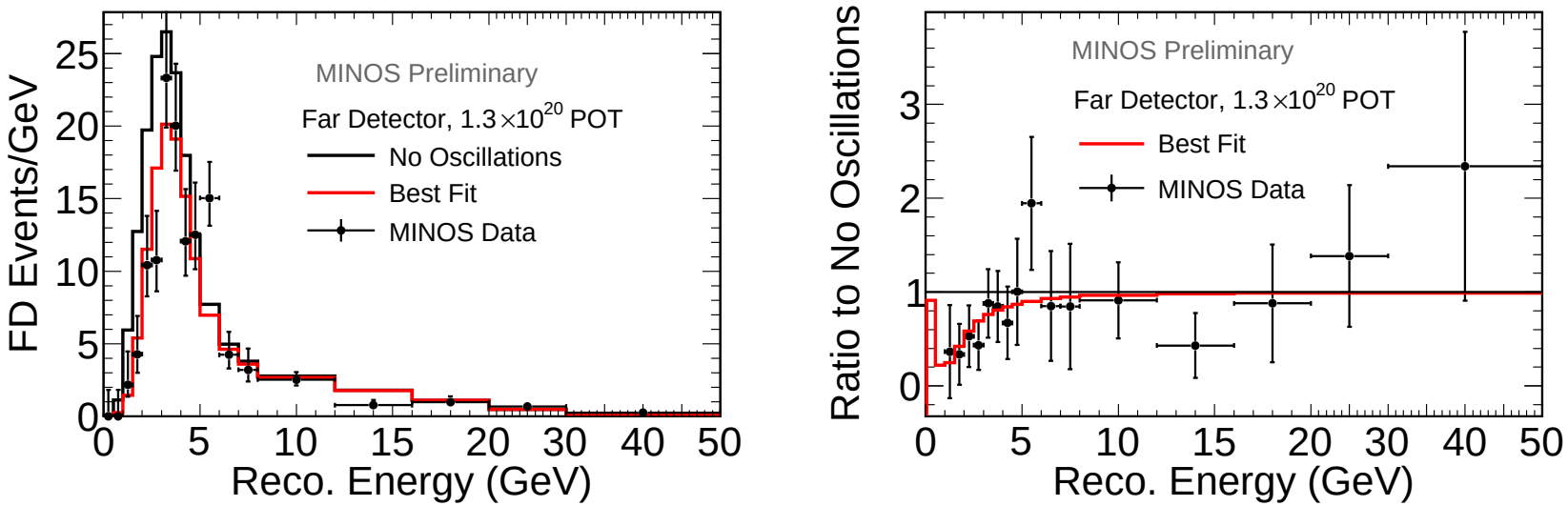

Figure 43: Left the far detector data, best fit, and no oscillation prediction. At right are the ratios of data and best fit to the no oscillation hypothesis. This is a temporary plot based on an MDC experiment so the formatting can be decided prior to box opening. minos-doc-7204

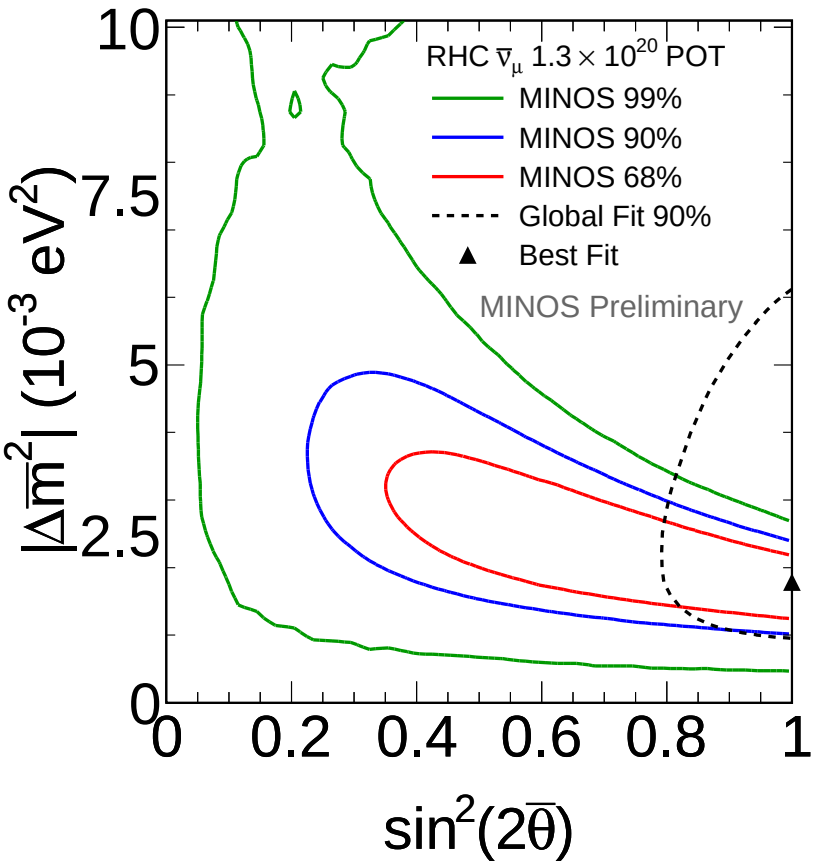

Figure 44: The 68%, 90%, and 99% antineutrino oscillation contours from RHC running. The contours are determined using the Feldman-Cousins method and include systematics. They are compared with the 90% global fit contour from Maltoni. This is a temporary plot based on an MDC experiment so the formatting can be decided prior to box opening. The wiggliness in the 99% contour is from low statistics in the Feldman-Cousins grid, also to be fixed prior to box opening. minos-doc-7204